

# Graphitic Carbon Nitride ( $g-C_3N_4$ ): A Proficient Electrode Material for Flexible Supercapacitors

Dipanwita Majumdar<sup>1\*</sup>, Rudra Sarkar<sup>2</sup> and Munmun Mondal<sup>3</sup>

<sup>1</sup>Department of Chemistry, Chandernagore College, Chandannagar, Hooghly, Pin-712136, West Bengal, India.

<sup>2</sup>Department of Chemistry & Chemical Biology, Indian Institute of Technology (Indian School of Mines) Dhanbad, Dhanbad-826004, Jharkhand, India.

<sup>3</sup>Department of Chemistry, Indian Institute of Technology, Kharagpur, Kharagpur-721302, West Bengal, India.

\*Correspondence to: Dipanwita Majumdar, Department of Chemistry, Chandernagore College, Chandannagar, Hooghly, Pin-712136, West Bengal, India. Email: [wbesdmajumdar@gmail.com](mailto:wbesdmajumdar@gmail.com)

Received: July 29, 2023; Accepted: November 30, 2023; Published Online: December 7, 2023

Citation: Majumdar D, Sarkar R and Mondal M. Graphitic Carbon Nitride ( $g-C_3N_4$ ): A Proficient Electrode Material for Flexible Supercapacitors. *Advanced Materials Science and Technology*, 2023;5(2):0519627.

<https://doi.org/10.37155/2717-526X-0502-3>

**Abstract:** In the recent years, graphitic carbon nitride ( $g-C_3N_4$ ), the metal-independent semiconductor, has captured immense interest in the field of supercapacitor technology owing to its numerous superior qualities together with layered morphology, unique physico-chemical features, ease of synthesis, low fabrication cost, environmental compatibility in addition to mechanical tenacity. Its' graphitic type double-bonded nitrogen-rich layered structure promotes large number of reactive regimes and effective binding sites that considerably boost the electrochemical activity compared to other widely known graphene analogues. Besides, the architectural distinctiveness in  $g-C_3N_4$  has introduced better designing opportunities for fabricating various types of nanocomposites with improved structural, electronic and electrochemical features. Thus, meticulously engineered  $g-C_3N_4$  electrode materials have displayed high electrochemical and mechanical tenacity, which have opened up new dimensions in the manufacturing of flexible supercapacitors with advanced technological applications. This review addresses these recent progresses of  $g-C_3N_4$  based systems in the electrochemical energy storage arena, embracing the current challenges faced and some of the prospects that are presumed to possibly emerge in the near future with this highly promising material.

**Keywords:** Two-dimensional; Graphitic carbon nitride; Charge storage; Supercapacitor; Semiconductor; Nanocomposite



© The Author(s) 2023. **Open Access** This article is licensed under a Creative Commons Attribution 4.0 International License (<https://creativecommons.org/licenses/by/4.0/>), which permits unrestricted use, sharing, adaptation, distribution and reproduction in any medium or format, for any purpose, even commercially, as long as you give appropriate credit to the original author(s) and the source, provide a link to the Creative Commons license, and indicate if changes were made.

# 1. Introduction

## 1.1 Current Status of Supercapacitors

Supercapacitor technology has drawn immense attention all around the globe to address the urgent need for a reasonable pricing, clean, renewable, and sustainable energy support in today's world<sup>[1]</sup>. Compared to trivial rechargeable batteries, supercapacitors are endowed with superior qualities of fast power supplying capacity (power density), eco-compatibility, and long lifetime along with mechanical durability. They can also be desirably miniaturized for constructing highly portable e-gadgets to back up the

energy demands in almost every sector of modern-day technology. Nonetheless, noticeable low charge storing capability (energy density), high self-discharging rates, and elevated production cost have severely restricted their massive commercialization<sup>[2]</sup>. Consequently, they are selectively employed in supplying electrical energy for short time period and in power backup gadgets, driving regenerative braking systems, and for rapid accelerations in hybrid electric vehicles (HEVs), serving mostly as auxiliary power distributing systems to minimize excessive stress on the batteries<sup>[3]</sup>.

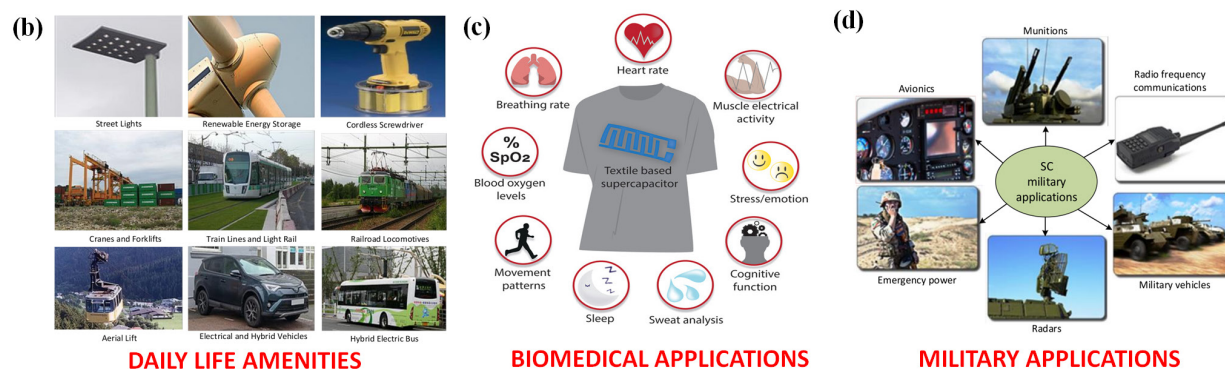
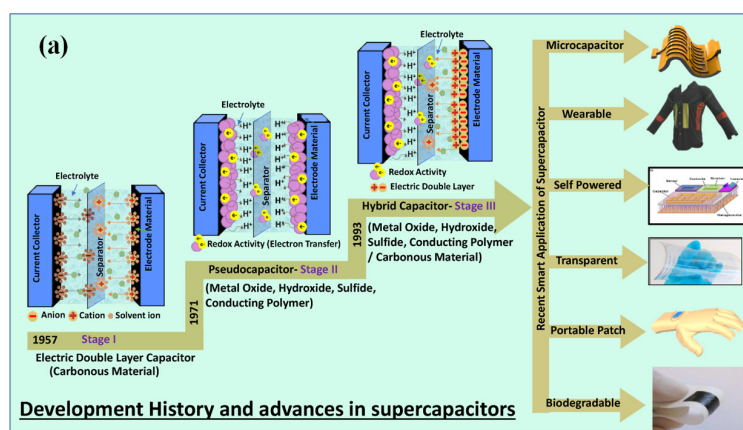


**Figure 1.** (a) Time-line of progress of supercapacitor technology Ref. [5] reproduced under the terms of the Creative Commons 4.0 CC BY license © 2022 The Authors. Licensee MDPI, Basel, Switzerland. (b-d) various application of flexible supercapacitors in vital sectors of modern-day events; (b) and (d) Ref. [6] © 2022 by the authors. Licensee MDPI, Basel, Switzerland under the terms and conditions of the Creative Commons Attribution (CC BY) license; (c) Ref. [8] reproduced under the terms of the Creative Commons 4.0 CC BY license © 2022 The Authors. *Advanced Science* published by Wiley-VCH GmbH

Nonetheless, rigorous simulation studies have comprehended that proper designing can considerably boost the overall energy storage characteristics in supercaps<sup>[4]</sup>. Accordingly, worldwide research has been continuously exploring the conditions for optimization of various parameters that may lead to designing

of cheap, smart, and intelligent supercapacitors for powering wearable and portable electronics in the near future<sup>[5]</sup>. With the advancement of time, studies perceived that the scheming of novel, versatile, and high-performing electroactive materials are mandated for accomplishing self-sustainable and

robust supercapacitors for commercial needs. **Figure 1a** highlights the chronological progress of supercapacitor science and technology based on designing and usage of various productive materials with diverse electrochemical energy storage mechanisms<sup>[6,7]</sup>. Currently, the scenario demands the easy devising of mechanically foldable energy storage systems with minimum maintenance and large stress adaptability, so that they can be extensively employed as important resources in the daily consumer electronics, e-transport facilities, as well as in the vital life-saving sectors of biomedical sciences, space engineering, and military applications, as outlined in **Figure 1b-1d** respectively<sup>[6-8]</sup>.

Thus, for indiscriminative expansion of such technological utilization globally, proper choice and designing of electroactive components are very crucial whose feasibility has been possible through the marvellous advancement of materials science, an immense boon for nourishing such intricate device fabrication processes<sup>[9-12]</sup>. With the advent of nanoscience and nanotechnology, several constructions of diversified architectures have been proposed, framed, and explored for accomplishing better electrochemical responses<sup>[10-12]</sup>. Since, the electrochemical charge storage and its conversion efficacy are principally guided by the nature, shape, morphology, and composition of the electroactive materials comprising the electrodes and their complementarity with the employed electrolytes, their judicious scheming, has

been the main challenge so far in this streaming field of research<sup>[13-18]</sup>.

Thus, before resuming our journey with the detailed discussion on the topic of the title, let us briefly outline the fundamentals and basic terminologies associated with the electrochemical energy storage science for better subject understanding and interpretation of the ideas. Accordingly, the important parameters that define the efficacy of the supercapacitors, have been delineated in the following section.

## 1.2 Basic Things to Know About Supercapacitors

The basic set-up of a typical supercapacitor comprises of two electrodes ionically connected by an electrolyte; the entire system being sealed in an insulating envelope. The efficiency of supercapacitors majorly relies on both electrode and electrolyte characteristics, as outlined in the **Figure 2a**<sup>[11]</sup>. In principle, the supercapacitor system acquires electrical energy in the form of the electric field i.e., the charge stored at the interface between electrodes and electrolytes as indicated in the **Figure 2b**.

To perceive the relative performances of these different designed materials and device constructions, it is essential to get introduced with some of the essential terminologies intimately associated with the supercapacitor technology, as defined in the **Table 1** and mathematically represented in the **Figure 2c** respectively.

**Table 1.** Essential terminologies associated to supercapacitor performance efficacy

| Parameter                                     | Description   |
|---|---|
| Specific capacitance                          | Charge storing capability per unit mass/area/volume of the material/ device   |
| Specific energy/ energy density               | Quantity of energy accumulated per unit mass or unit area or unit volume of the desired system  |
| Specific power/ power density                 | Amount of energy delivered per unit mass or unit area or unit volume of the systems   |
| Rate capacity or capability                   | Capacitive response variation at different current densities or scanning voltages, to justify the power-generating efficacy of the system at large applied currents with minimum voltage fall   |
| Electrochemical reversibility                 | Deals with the extent of reversible nature of the charge transfer reactions taking place at the electrode/electrolyte interfaces.   |
| Potential window                              | Specifies the voltage range within which the system, namely, the electrode and electrolyte, undergoes no irreversible oxidation/ reduction nor any kind of perpetual electrochemical disintegration.  |
| Electrochemical stability/ cyclic performance | The reversibility in material/ device capacitance at a specific voltage range, recorded at constant current or potential scans rates. It is determined by the capacitance retention efficacy of the material/device for large numbers of Galvanostatic Charging/Discharging (GCD) cycles. |
| Coulombic efficiency or faradaic yield        | Represents the efficacy of charge transfer within a system originating from an electrochemical reaction. It is obtained by the difference between the calculated and observed electrode voltages essential for driving the electrochemical reaction at the desired rate.                  |

| Parameter                          | Description  |
|------------------------------------|--|
| Equivalent series resistance (ESR) | It signifies the system resistances linked with various components, each performing analogous to an electrical unit where the electrode double layer is compared as a capacitor and the electrolyte resistance to a resistor respectively. It is calculated from GCD curves and EIS studies. |

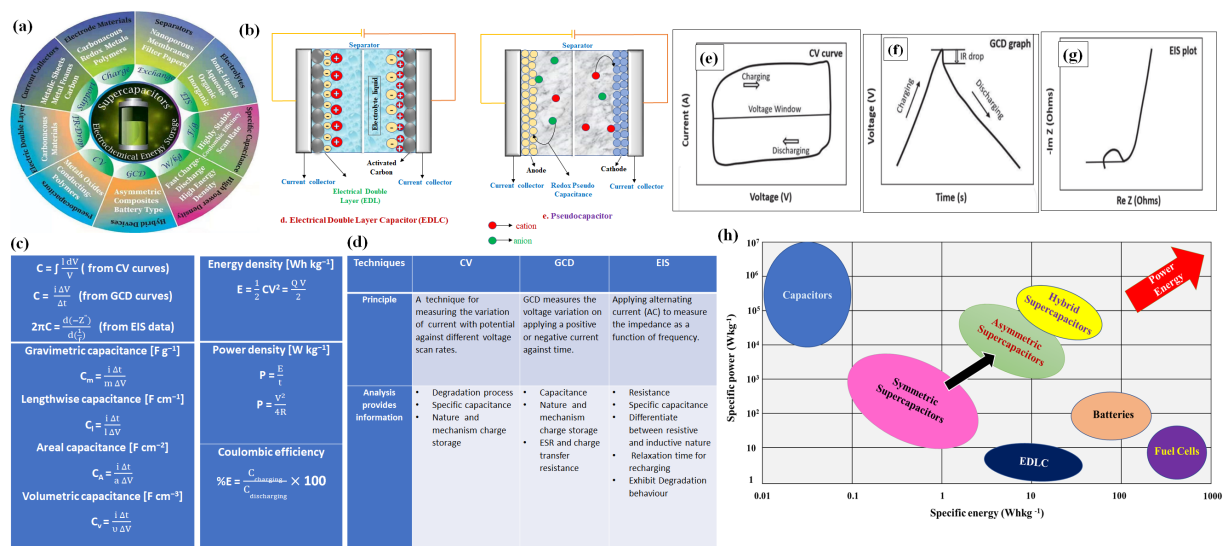


**Figure 2.** (a) Essential efficacy determining components of supercapacitors Preproduced from Ref. [11] under the terms and conditions of the Creative Commons Attribution 4.0 (CC BY) license © 2021 by the authors. Licensee MDPI, Basel, Switzerland, and (b) popular mechanism of storage of charge in these devices; (c) Formulae representing the calculations of various important parameters outlined in **Table 1**; (d) Outline of the working principles and associated information on electrochemical features of supercapacitor electrodes obtainable from CV, GCD and EIS techniques and (e-g) represents the typical signatures of CV, GCD and EIS (Nyquist plot) respectively for supercapacitive materials. Preproduced from Ref. [19] under the terms and conditions of the Creative Commons Attribution 3.0. (CC BY) license © 2021 by the authors. Licensee IntechOpen; (h) A Typical Ragone plot showing the variation of specific energy with specific power for different energy storage systems

Most of the above-stated parameters such as specific capacitance, equivalent series resistance (ESR), charge transfer resistance, energy and power densities, coulombic efficiency, etc., as indicated in the **Figure 2c and 2d** and defined in **Table 1** are usually obtained experimentally from the data procured from Cyclic Voltammetry profiles (CV), Galvanostatic Charging / Discharging (GCD) graphs and Electrochemical Impedance Studies (EIS) respectively. **Figure 2e-2g** shows characteristic nature of the CV plot (pseudo-rectangular), GCD curve (triangular) and Nyquist plot (semi-circular with a long tail obtained from EIS data) generally observed for supercapacitive materials<sup>[8,19,20]</sup>. To obtain a clear-cut idea on their relative performances and commercial significance of the designed material or device or both, a Ragone plot is often drawn with the logarithmic values of specific energy ( $W \cdot h \cdot kg^{-1}$ )/

energy density ( $W \cdot h \cdot cm^{-2}$ /  $W \cdot h \cdot cm^{-3}$ ) and specific power ( $W \cdot kg^{-1}$ )/power density ( $W \cdot cm^{-2}$ /  $W \cdot cm^{-3}$ ), as pictorially indicated in the **Figure 2h**. High values of specific power and specific energies are the main objectives of these energy storage systems that has to be accomplished.

On the basis of charge storing mechanistic process, supercapacitor electrode materials have been classified as electrochemical double layer capacitive (EDLC) and pseudocapacitive (PC) materials respectively<sup>[21]</sup>. The EDLC type materials such as mesoporous carbons, graphenes, CNTs, etc., storage charge through formation of double-layer capacitance at the electrode/ electrolyte interface<sup>[22-24]</sup>. The electric charges accumulate on the electrode surfaces while the ions of opposite charges remain on the electrolyte side. Such materials generally show high

electrochemical reversibility and stability in different electrolyte media. Further, EDLC materials are bestowed with qualities such as light weight, larger abundance and easy availability, large surface area, high electrical conductivity, exceptional chemical stability and ultrafast charging/ discharging kinetics. On the other hand, PC materials, for instance, metal-based compounds including oxides/ nitrides/ chalcogenides, *etc.*, involve charge storage via capacitive Faradaic processes involving charge transfer between electrode and electrolyte<sup>[25]</sup>. PCs have greater charge storing capacity, much closer to the desired values commercially demanded but sincerely lack electrochemical stability like EDLCs<sup>[26]</sup>. Thus, current fabrication approach stands in improving the persisting demerits of EDLCs and PCs in individual perspective as well as propose composite materials through hybridizing them in appropriate proportions to introduce synergic materialistic improvement which can comprehensively modify their electrochemical potentialities at appreciable extent so that the designed materials can be placed in the extreme upper right part of a typical Ragone plot<sup>[4,27]</sup>. However, it is vital to note that, such designing would be significantly fruitful only on successful upgradation of the intrinsic features in the individual components forming the nanocomposite<sup>[28-31]</sup>.

### 1.3 Specialty of Layered Materials in the Supercaps Fabrication

As far as scheming of electroactive stretchable electrodes for driving wearable electronics are concerned, scientific assessments apprehended the appreciable outcomes from graphenes based supercapacitors as well as the rigorous studies with layered metallic chalcogenides, nitrides, carbides, and analogues in energy conversion and storage applications which made the explorations of the 2D layered nanomaterials more dominant than ever before in this area of research<sup>[32]</sup>. Their uniqueness in providing large surface areas, high theoretical capacitance, structural anisotropy, high charge mobility and tunable bandgaps, mechanical durability, and facile synthesis benefits, have made their frontiers in this technological arena. Its atomically thin large aspect ratio ensures remarkable behaviours relative to its bulk with novel features owing to quantum confinement. The ultra-thin morphology facilitates shorter distances for electrons leading to a very high charge carrier mobility

and ultra-high electrical conductivity. Additionally, enhanced transverse area also provides larger number of surface atoms for improved physicochemical environment. Thus, the current challenge lies vastly in fabricating appropriate scalable synthetic strategies that would yield smart and stable 2D materials with advanced activities<sup>[33]</sup>.

### 1.4 Why Focusing on Improving the Qualities of 2D EDLC Carbon-based Nanomaterials?

The EDLCs play a significant role in providing charge transport facilities, structural flexibility, and skeletal support for designing of heterostructures with varieties of organic and inorganic semiconductors with high pseudocapitance. However, these nanomaterials suffer from an intrinsic aggregation tendency, which dramatically reduces ion transport and accessibility to the surface. Thus the quality of the 2D EDLC nanomaterials demands serious restoration in their structural features which again highly influences the electrochemical property. Especially during electroactive material fabrication, the following important qualities are mostly shouldered by them in the resultant hybrid structure:

- Long life period of operation;
- Good electrochemical reversibility;
- Simple charging procedure;
- High charging and discharging kinetics;
- Simple and low production cost;
- Improved safety and eco-compatibility;
- Responsive towards different varieties of electrolytes;
- Very low internal resistance.

Thus, designing of superior EDLCs can substantially upshot the prospect of formation of high-quality electroactive materials with innovative attributes to the energy sector.

### 1.5 Popular 2D EDLC Nanocarbons as Supercapacitive Materials

For the past few decades, popular EDLC nanocarbons such as nano-graphite flakes, functionalized graphenes, carbon nanotubes, fullerenes, activated carbons, mesoporous carbons, and others, as depicted in the **Figure 3a**, including naturally obtained or synthetically prepared derivatives have controlled the EDLC sector owing to their outstanding cyclic performance<sup>[34]</sup>. Hence, to meet the marketable needs in terms of

exhibiting upgraded capacitive responses, better 2D nanocarbons have been looked for by the scientists.

Graphene, ever since its discovery as one of the most popular allotropic forms of carbon, has dominated the “post-silicon electronics” primarily by virtue of its stimulating amalgamation of electrical conductivity, and mechanical stability<sup>[35]</sup>. Accordingly, it has been

the most widely explored EDLCs in the field of supercapacitor technology. Several strategies have been framed to widen up the band gap of semi-metallic graphene through necessary physical, chemical, and electrochemical modifications, introduction of defects through deletion of carbon atoms, or the incorporation of heteroatoms, *etc.*<sup>[36]</sup>

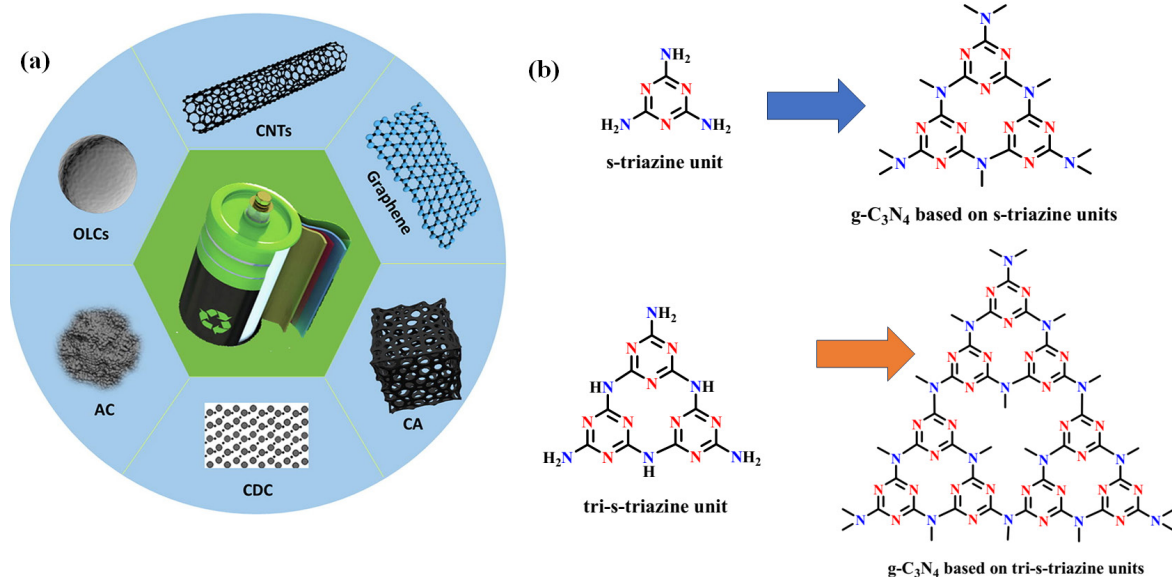


**Figure 3.** (a) Commonly used nanocarbon electrode materials such as carbon nanotubes (CNT), graphene, activated carbons (AC), onion-like carbons (OLC), carbide-derived carbons (CDC) in supercapacitor technology. Ref. [34] reproduced under the Creative Commons 4.0 CC-BY-NC-ND license © 2022 The Authors. Published by Elsevier Ltd.; (b) Chemical structures of s-triazine and tri-s-triazine forming the primary building units of 2D layers of g-C<sub>3</sub>N<sub>4</sub>

Nonetheless, rigorous and systematic interpretation have conferred that the high electrical conducting graphene electrodes in pristine phases considerably lack adequate surface properties due to severe layer stacking issues, which drastically lower their surface area and thus EDLC charge storage propensity. Therefore, existing situations mandate necessary modifications such as surface engineering, heteroatom(s) doping, heterojunction formation, and so on for compulsory upgradation of the material capabilities<sup>[37,38]</sup>.

To begin with the simplest strategy i.e., the process introduction of heteroatoms (such as O, N, B, S, and P, *etc.*) through the process of doping in the nanocarbon skeleton has exhibited great potentiality in augmenting the capacitance through additional pseudo-capacitance contribution mediated by surface faradaic processes<sup>[39]</sup>. The presence of additional electron density, modified the donor-acceptor characteristics of these nanocarbon

materials, resulting in an improved pseudocapacitive charge transfer process. Besides, judicious surface functionalization also facilitates good binding and strong adhesion to the current collector surface which is vital for smooth delivery of interfacial current for driving heavy duty electrical appliances<sup>[40]</sup>. Nitrogen doping, so far, among all others, has proved to be an utmost beneficial approach owing to ease of availability of suitable precursors, modified electronic structure with improved provision for electrical charge transfer via minimization of work function, increased Lewis base characteristics, boosted surface reactivity as well as material wettability towards polar solvents; all these attractive factors cumulatively promoting the overall capacitive performance considerably<sup>[41]</sup>.

Nonetheless, rigorous investigations have unveiled many critical shortcomings which have enforced second opinion regarding implementation of this

procedure. Homogeneous nitrogen doping process can involve intricate procedures and post-treatments, with poor turnover and accompanied by the production of toxic by-products. Further, functional moieties can only be incorporated on the surface of carbon materials while a significant bulk segment remains in unaffected conditions. Additionally, it has been justified that such procedures often cause random disruption of morphology which leads to structural and physical damages of the 2D carbon lattice, besides deteriorating the associated properties (e.g., structural rigidity, charge mobility) in pristine phases<sup>[42]</sup>. Another vital question arises regarding the homogeneity as well as the low production yield of the functionalized nanocarbons such as graphenes or their nanocomposites relative to precursors which considerably augments their manufacturing cost. Most of the functionalized graphenes including aerogels or 3D porous architectures, *etc.*, originates from the graphene oxide, the synthesis, and reproducibility, of the latter is a serious challenge with the functional moieties not often well-organized but randomly distributed on the layer surfaces and under such situation, as obviously expected, should not be profitable for the fruitful formation of the desired nanocomposite with acceptable features<sup>[43-46]</sup>. There lies the urge for better, more accessible, and convenient modes of fabricating structurally modified nanocarbon electrode materials for the next generation supercapacitors.

## 2. Unique Features of Graphitic Carbon Nitride

Graphitic carbon nitride (g-C<sub>3</sub>N<sub>4</sub>), a metal-free

polymeric, 2D graphite-like, conjugated semiconductor material, which was discovered as early as 1834, started its application-based scientific journey only in the early 21<sup>st</sup> century with the discovery of its photocatalytic properties for hydrogen evolution process. Since then, graphitic carbon nitride (g-C<sub>3</sub>N<sub>4</sub>), has turned out to be a hot spot in several technological findings especially in the fields of catalysis, hydrogen storage, atmospheric and aquatic decontaminations, solar energy harvest and conversion, *etc.*, owing to its well established chemical composition, tuneable structural characteristics along with exclusive properties by virtue of its rich nitrogen content, extraordinary physicochemical prospects, unique optoelectronic features, eco-compatibility, and simpler fabrication procedures<sup>[47]</sup>. Thus, the above-mentioned distinctive features have rightly prompted its applicability in the enthralling field of electrochemical charge storage and conversion technology.

The material g-C<sub>3</sub>N<sub>4</sub> has been coined the term “graphitic carbon nitride” owing to its structural resemblance with the layer-structured graphite systems comprising of stacked sheets of sp<sup>2</sup> carbons arranged in hexagonal crystal structure<sup>[48]</sup>. Nonetheless, it definitely possesses some uniqueness which have placed it in a better position in the group of EDLCs till date. Unlike graphite or graphenes, it consists of exclusive covalently-linked, sp<sup>2</sup>-hybridized carbon and nitrogen atoms arranged in an alternating fashion, replacing every other carbon with nitrogen in the basic honeycomb motif of the graphene lattice. A comparative study of the features of graphite and graphitic carbon nitride has been placed in the **Table 2** to give a better idea of the above stated fact<sup>[47-49]</sup>.

**Table 2.** Comparative study of some of the important aspects of 2D carbon nanomaterials

| Characteristics                    | Graphite   | Graphitic carbon nitride   |
|------------------------------------|--|--|
| Structure                          | Stacked layers of planes with all $\pi$ -conjugated sp <sup>2</sup> carbons arranged in 2D honeycomb structure | 2D graphite type structure with a nitrogen substituted framework which exhibits pi conjugation with sp <sup>2</sup> hybridization of carbon and nitrogen atoms in each plane remaining in stacked layers |
| Interlayer distance                | 0.335 nm   | 0.315 nm   |
| Packing of layers                  | Less dense packing   | More intensely packed layers   |
| Quantum capacitance                | Low  | High   |
| Conductivity                       | Metallic   | n-type semiconductor   |
| Chemical stability                 | Not soluble in any acidic, alkali or other organic solvents  | Not soluble in any acidic, alkali or other organic solvents  |
| Wettability                        | Poor   | High   |
| Aptitude towards functionalization | Low  | High   |
| State                              | Grey powder  | Yellow coloured polymeric powder (bulk), pale yellow in nanophase  |

Out of the several phases of carbon nitrides, the g-C<sub>3</sub>N<sub>4</sub> shows stacked 2D layered morphology comprising of tri-s-triazine building unit, as depicted in the **Figure 3b**, being the most widely accepted basic unit rather than the triazine-based analogue, former being more thermodynamically favoured phase as revealed from experimental and theoretical findings in the recent past. Such unique arrangement introduces homogeneous distribution of triangular nanopores unlike the honeycomb structure typical in graphite or graphene layers<sup>[47]</sup>.

Apart from the above characteristics, substitution by more electron-rich nitrogen into the hexagonal carbon network furnishes additional delocalized  $\pi$ -electrons that modifies the electronic states as well as facilitates improved charge transfer kinetics, similar to that targeted for functionalized graphenes produced after necessary and rigorous structural engineering<sup>[47]</sup>. Heteroatom substitution has also prompted widening of the band gap compared to perfect graphite or graphenes as verified from Density Functional Theory (DFT) and spectroscopic analysis. In contrast to nano graphite or multi-layered graphenes, the smaller stacking space between the aromatic layers in g-C<sub>3</sub>N<sub>4</sub> as a result of stronger inter-sheet binding ensures greater packing density as well as faster charge transport property perpendicular to the planes than the former ones. Moreover, the in-plane hole appearance containing regular 'lattice holes' or 'atomic deletions' within the structure that equip the nanosheets with greater number of active edges and diffusion channels, resulting in a tremendous enhanced mass charge transfer rates as well as diverts aggregation to larger extent<sup>[50]</sup>. Furthermore, relative to less polar carbons, nitrogen-containing nanocarbons are found to demonstrate improved wettability in presence of different solvents that support faster ion transportation processes across the electrode material thus benefiting the material's capacitive performance.

Thus, research findings in the late years have repeatedly demonstrated g-C<sub>3</sub>N<sub>4</sub>, as an emerging and highly potential candidate for framing highly flexible supercapacitor electrodes with tunable surface area, charge accumulating capacity, rapid charge transmission, and improved accessibility towards electrolytic interaction. The system has been adequately bestowed with advantageous features in terms of

mechanical, electronic, and electrochemical properties besides possessing facile tailorable morphology, simple and cost-effective synthesis procedures compared to the other widely popularized graphene analogues. Consequently, the aim of this current review is to highlight the recent developments accomplished in the supercapacitor technology based on g-C<sub>3</sub>N<sub>4</sub> electrode systems, particularly its superiority observed relative to other traditionally employed nanocarbons, which might open up new doors towards a more sustainable future without impairing our environment.

### 3. Synthesis Approaches of Electroactive Graphitic Carbon Nitrides

Graphitic carbon nitride has been conveniently prepared via both top-down as well as bottom-up strategies as outlined in the **Figure 4**. Popular top-down approaches include exfoliation techniques from bulk phases while bottom-up methods include chemical processes such as pyrolysis, thermal vapor condensation and deposition as well as supramolecular preorganization procedures to yield various types of nanoarchitectures like nanofilms, sheets, fibers/tubes, *etc.* of the graphitic carbon nitride. Even template-based techniques are being employed to obtain desired shapes of the nanomaterial aimed for specific applications<sup>[42,49,51]</sup>. The products obtained via different approaches vary in their grain size, pore volume, and surface area which significantly influence the physiochemical properties of g-C<sub>3</sub>N<sub>4</sub> nanomaterial. Moreover, a number of factors such as nature of precursor, pyrolysis temperature, heating rates, solvents, *etc.* considerably control the yield and nature of the product formed in each process. Studies reveal that each of these precursors produces C<sub>3</sub>N<sub>4</sub> samples with varying conjugation degrees and defects density which again results in different degrees of electrochemical responses.

It is well generalized that bottom-up synthetic strategies offer better opportunities for structural control of nanomaterials compared to the top-down approaches. As far as g-C<sub>3</sub>N<sub>4</sub> synthesis is concerned, the simple and low costing, bottom-up strategies are more popular in contrast to the graphene or other 2D nanocarbons where the top-down approaches are more cost-effective. As a consequence, the opportunities for actually control of structure and functionalities are thus very narrowed. Thus, well-defined strategies that



confirm the yield of high quality and scalable quantity of  $g\text{-C}_3\text{N}_4$  nanostructures with smart properties are highly urged<sup>[50-54]</sup>.

Accordingly, this realization has triggered continuous hunt and strong desire for simple and

productive electrode materials bestowed with tuneable electrochemical properties that have resulted in fast and vast explorations of versatile material  $g\text{-C}_3\text{N}_4$  (graphitic carbon nitride) in the field of supercapacitor technology for the last few years.

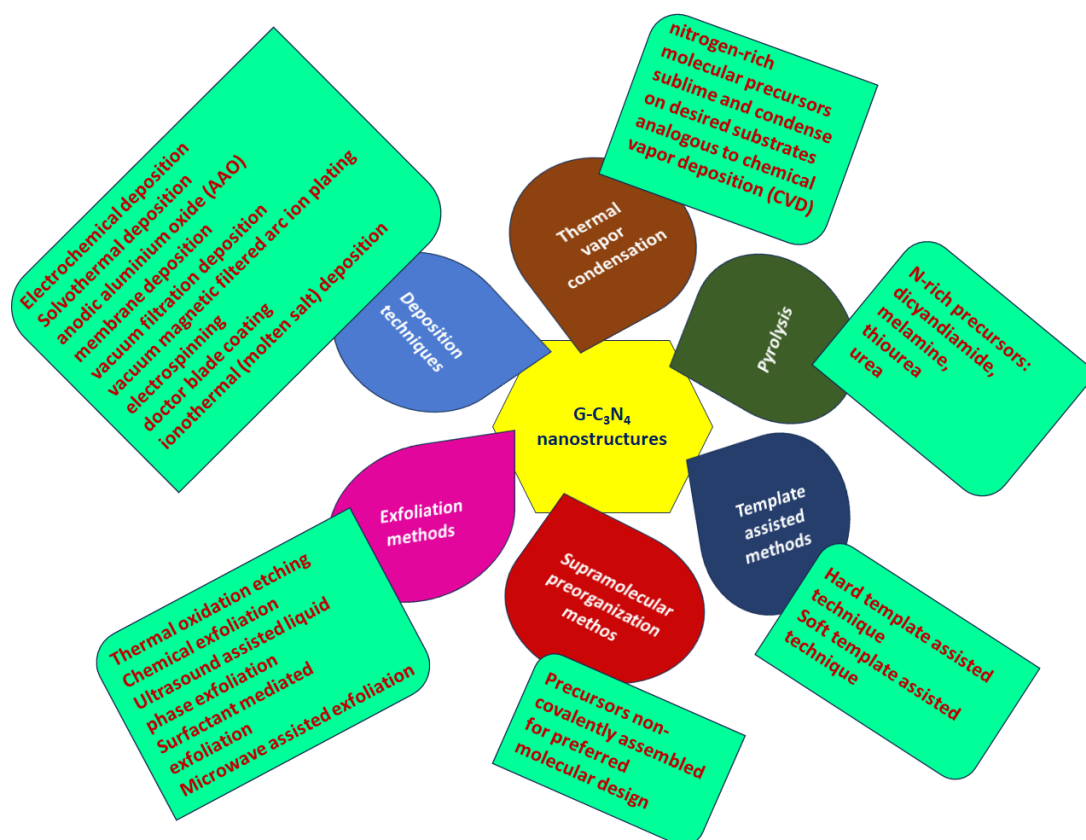


Figure 4. Common methods of designing  $g\text{-C}_3\text{N}_4$  nanostructures

#### 4. Supercapacitive responses of graphitic carbon nitride electrodes

As far as supercapacitor performance is concerned, nanophase materials are superior to their bulk counterparts owing to their larger specific surface area that increases the accessibility to more active sites for reaction, shortens the ions diffusion pathways, and increases the electrochemical aptitudes of the charge carriers. Simplistic fabrication strategies of  $g\text{-C}_3\text{N}_4$  via chemical routes have opened up new horizons in tailoring the morphology to accomplish better electrochemical signatures<sup>[55]</sup>. Accordingly, a number of controlling factors such as synthesis conditions and precursors, nature of dopants, appropriate functionalization, *etc.*, have significantly influenced the electrochemical responses of these nanomaterials. Consequently, various methodologies have been

adopted by researchers to systematically study and analyse their influences on the structure and capacitive outputs.

##### 4.1 Mode of Fabrication of Graphitic Carbon Nitride Nanostructures

As previously stated, the synthesis conditions considerably influence the structure and hence electrochemical properties of the synthesized graphitic carbon nitride as indicated in the **Table 3**<sup>[56-62]</sup>. Thus, the nature of starting precursors and the mode of synthesis of the graphitic carbon nitride is very crucial to apprehending its electrochemical output compared to other nanocarbon varieties. The simplest and reproducible technique, irrespective of low yield reports, involves pyrolysis of urea/thiourea, as it can be executed over a wide temperature range (from 450 °C to 600 °C) in conventional ovens

without the need for inert atmosphere conditions. However, the so-obtained g-C<sub>3</sub>N<sub>4</sub> samples via direct polycondensation procedures are commonly in the bulk form with exceptionally poor surface area<sup>[10, 63]</sup>. Hence, supplementary strategies including oxidative/ strong acid assisted delamination, exfoliation techniques with the aid of thermal, ultrasound, microwave energies; template-assisted as well as template-free synthesis procedures, have been popularly adopted to bring them into nanophase for improving their porous nature, surface area, and other morphological features. Again, the variety formed using cyanamide and dicyanamide generally suffer from low solubility and thus further processability becomes a big question<sup>[64]</sup>. Moreover, cyanamide is very expensive and relatively explosive in nature, and so to cope up with this problem, Xu group<sup>[65]</sup> proposed the employment of a water-soluble, environmentally friendly, and cheap material in the form of guanidine hydrochloride, to serve as a better

option for the preparation of g-C<sub>3</sub>N<sub>4</sub>. Parallely, in bottom-up approach, judicious assembling of melamine precursor and triazine derivatives using the aid of supramolecular preorganization linkages followed by calcination resulted in the formation of g-C<sub>3</sub>N<sub>4</sub><sup>[66]</sup>. In another approach, combinations of coal tar pitch, urea and KOH at an activation temperature of 600 °C resulted in the formation of high nitrogen content (7.06 at %) based N-doped porous carbon nanosheets with augmented specific surface area (1181 m<sup>2</sup> g<sup>-1</sup>) that resulted in remarkable capacitive responses (210 F g<sup>-1</sup> @ 0.1 A g<sup>-1</sup>) due to the large pseudocapacitance contribution of the N doping. The unique architecture also promoted exceptional rate capacity and cycling stability. These EDLCs electrodes on assembling to form symmetric supercapacitor recorded noticeable energy density of 7.15 Wh kg<sup>-1</sup> with a capacitance retention efficacy of 91.2 % even after 5000 cycles @ current density of 1 A g<sup>-1</sup><sup>[67]</sup>.

**Table 3.** Factors influencing the electrochemical responses of graphitic carbon nitride

| Factors influencing              | Materials   | Carbon-nitride source, synthesis methods                           | Electrolyte (operating potential range in Volts) | Specific capacitance (F g <sup>-1</sup> ) [at current density (A g <sup>-1</sup> )] | Cycle number, capacitance retention (%) | Specific energy E (Wh kg <sup>-1</sup> ) | Specific power P (W kg <sup>-1</sup> ) | Ref. |
|----------------------------------|---|--|--|---|---|--|--|------|
| Morphology and synthesis methods | g-C <sub>3</sub> N <sub>4</sub> nanofibers                  | Melamine   | Na <sub>2</sub> SO <sub>4</sub> (0.1-0.7)        | 263.75 (0.1)  | 2000, 93.6%                             | /  | /                                      | [56] |
|                                  | Tubular g-C <sub>3</sub> N <sub>4</sub> based carbon fibers | Melamine   | KOH (-0.2-1)                                     | 233 (0.2)   | 1000, 90%                               | /  | /                                      | [57] |
|                                  | Activated carbon nitride (ACN)                              | Melamine, pyrolysis or activation                                  | [BMIm] BF <sub>4</sub> / acetonitrile (-1.3-1.3) | 185 (0.5)   | 5000, 87.2%                             | 16.9                                     | 650                                    | [58] |
|                                  | Exfoliated g-C <sub>3</sub> N <sub>4</sub>                  | Urea, pyrolysis  | LiClO <sub>4</sub> (0.2-0.8)                     | 113.7 (0.2)   | 5000, 89.3%                             | 76.5                                     | 11.9                                   | [59] |
|                                  | Mesoporous graphitic carbon nitride (MGCN)                  | Melamine, carbonization  | H <sub>2</sub> SO <sub>4</sub> (-0.2-0.8)        | 244 (0.5)   | 5000, 100%                              | 30                                       | 4                                      | [50] |
|                                  | g-C <sub>3</sub> N <sub>4</sub> hollow nanocubes            | Calcining cyanuric acid-melamine in presence of potassium chloride | Na <sub>2</sub> SO <sub>4</sub> (0-0.8)          | 10.44 mF cm <sup>-2</sup> (0.05 mA cm <sup>-2</sup> )                               | 2500, 100%                              | 25 μWh cm <sup>-3</sup>                  | 17 mW cm <sup>-3</sup>                 | [60] |
| Effect of doping                 | Oxygen doped g-C <sub>3</sub> N <sub>4</sub> (GOOCN)        | Melamine, solution-based method                                    | H <sub>2</sub> SO <sub>4</sub> (-0.8-0)          | 265 (1)   | 5000, 94%                               | 36.45                                    | 2.5                                    | [62] |
|                                  | Red phosphorus g-C <sub>3</sub> N <sub>4</sub>              | Melamine, mechanical ball milling                                  | Na <sub>2</sub> SO <sub>4</sub> (0-0.4)          | 465 (1)   | 1000, 90%                               | /  | /                                      | [61] |

Further, soft template technique has been employed for the synthesis of mesoporous graphitic carbon

nitride in the recent past. Such a challenging task was successfully handled by direct carbonization of methylated surfactant-polymer composite to form the graphitic carbon nitride material. The resultant electroactive system established outstanding capacitive responses, including gravimetric capacitance as high as  $279 \text{ F g}^{-1}$  @  $0.25 \text{ A g}^{-1}$  current density, high rate-capability, appreciable cycling stability, and 100% coulombic efficiency over 5000 cycles using  $1 \text{ M H}_2\text{SO}_4$  electrolyte. Such remarkable capacitive response was attributed to the large surface area that exposed more active sites for charge storage, easily accessible mesoporous structure that shortened ions diffusion path distance and high density of pyridinic nitrogen content that enhanced the overall capacitance through surface-mediated Faradaic charge transfer process<sup>[68]</sup>. Investigations also reveal that surfactants' nature has been an essential criterion in tailoring the textural properties of mesoporous graphitic carbon nitride as well as controlling the polycondensation process, the C/N ratio and surface functionalities in these mesoporous graphitic carbon nitride systems<sup>[69-70]</sup>. Accordingly, three different surfactants, namely, cationic (cetyltrimethylammonium bromide, CTAB), neutral (polyethylene glycol p-(1,1,3,3-tetramethylbutyl)-phenyl ether, Triton X-100) and anionic (sodiumdodecylsulphate, SDS) were employed to study their impact on the capacitance response of mesoporous graphitic carbon nitride systems. Among them, the highest gravimetric capacitance was observed as high as  $279 \text{ F g}^{-1}$  @ current density of  $0.5 \text{ A g}^{-1}$  for the sample synthesized using Triton X-100 surfactant, which was ascribed to larger surface area, greater density of mesopores with larger pore volume and increased surface functionalities. Asymmetrical supercapacitor devised using this superior material delivered specific energy of  $20.97 \text{ Wh kg}^{-1}$  @ specific power of  $499.94 \text{ W kg}^{-1}$  along with excellent cyclic stability, much superior to the values reported for various nitrogen-doped carbonaceous materials<sup>[69]</sup>.

#### 4.2 Influence of Morphology of g-C<sub>3</sub>N<sub>4</sub>

Tuning of structural features to yield larger surface accessible area, broad channels for smooth ion insertion/ de-insertion roadways as well as extended electronic conduction networks considerably influence the electrochemical responses. Thus, appropriated

morphology is aimed to crop high discharge efficiency, rate capacities without any fall in cycle performances. Accordingly, Tahir and co-workers framed dense and uniform morphology-based g-C<sub>3</sub>N<sub>4</sub> nanotubes by reacting melamine and ethylene glycol in HNO<sub>3</sub>, followed by thermal annealing at  $450 \text{ }^\circ\text{C}$ <sup>[57]</sup>. Such one-dimensional g-C<sub>3</sub>N<sub>4</sub> tubes displayed larger surface area that boosted the specific capacitance to an appreciable value of  $233 \text{ F g}^{-1}$  at current density  $0.2 \text{ A g}^{-1}$  in  $6 \text{ M KOH}$  aqueous electrolyte, much higher than many common EDLC materials available in the literature. They also reported formation of template-free, one-dimensional g-C<sub>3</sub>N<sub>4</sub> nanofibers via a green and facile route, as indicated in the **Figure 5a and 5b**, exhibiting surface area almost 40 times higher than the bulk phase, recorded from the adsorption isotherm shown in **Figure 5c**. Such larger surface area exposure facilitated smooth electrode-electrolyte interface contact and accordingly improved the mass transfer kinetics and electrochemical responses to substantial extent. Therefore, the resultant nanofibers-based electrode showed much improved cyclic stability relative to the bulk counterpart, even at high current densities, as depicted in the **Figure 5d**. The framed electrodes with this smart electroactive material recorded high specific capacitance of  $263.75 \text{ F g}^{-1}$  along with appreciable rate capacity and decent cyclic performance of ~94% for 2000 successive charging/ discharging cycles @  $1 \text{ A g}^{-1}$  current density in  $0.1 \text{ M Na}_2\text{SO}_4$  aqueous electrolyte<sup>[56]</sup>. In another attempt, Liang *et al.*<sup>[71]</sup> obtained films of N-enriched mesoporous carbon nanofibers via electrospinning technique using graphitic carbon nitride (g-C<sub>3</sub>N<sub>4</sub>) nanosheets both as sacrificial template and N-doping source. The resultant electrode film displayed high N-doping level of 8.6 wt.% and increased specific surface area of  $554 \text{ m}^2 \text{ g}^{-1}$  that favoured notable augmentation of capacitive response, thus demonstrating gravimetric capacitance as high as  $220 \text{ F g}^{-1}$  @ current density of  $0.2 \text{ A g}^{-1}$ , rate capability (70% capacitance retentivity @ high current density of  $20 \text{ A g}^{-1}$ ), much superior to that of similarly prepared microporous carbon nanofiber film prepared without using g-C<sub>3</sub>N<sub>4</sub> nanosheets ( $145 \text{ F g}^{-1}$  @ current density  $0.2 \text{ A g}^{-1}$  along with 45% capacitance retentivity @ current density of  $20 \text{ A g}^{-1}$ ). Moreover, the fabricated electrode system showed enhanced electrochemical stability at a high current density as well as recorded

high specific energy when assembled to form a symmetrical supercapacitor ( $12.5 \text{ Wh kg}^{-1}$  @ specific power of  $72 \text{ Wh kg}^{-1}$ )<sup>[71]</sup>.

To upgrade the specific energy / energy density of the g-C<sub>3</sub>N<sub>4</sub> supercapacitors, Ghanem *et al.*<sup>[70]</sup> fabricated two-dimensional carbon nitride nanosheets via cost-effective thermal polymerization technique in aid with urea that exhibited outstanding electrochemical performance with a very wide operating voltage

window in 0.5 M H<sub>2</sub>SO<sub>4</sub> electrolyte. The assembled symmetric supercapacitor constructed with the resultant mesoporous electroactive material recorded ultrahigh specific energy of  $19.33 \text{ Wh kg}^{-1}$  at specific power  $499.9 \text{ W kg}^{-1}$  as well as displayed excellent electrochemical stability even after undergoing continuous 21,000 charging/ discharging cycles, superior to many other asymmetric and symmetrically assembled supercapacitors available in the literature<sup>[70]</sup>.

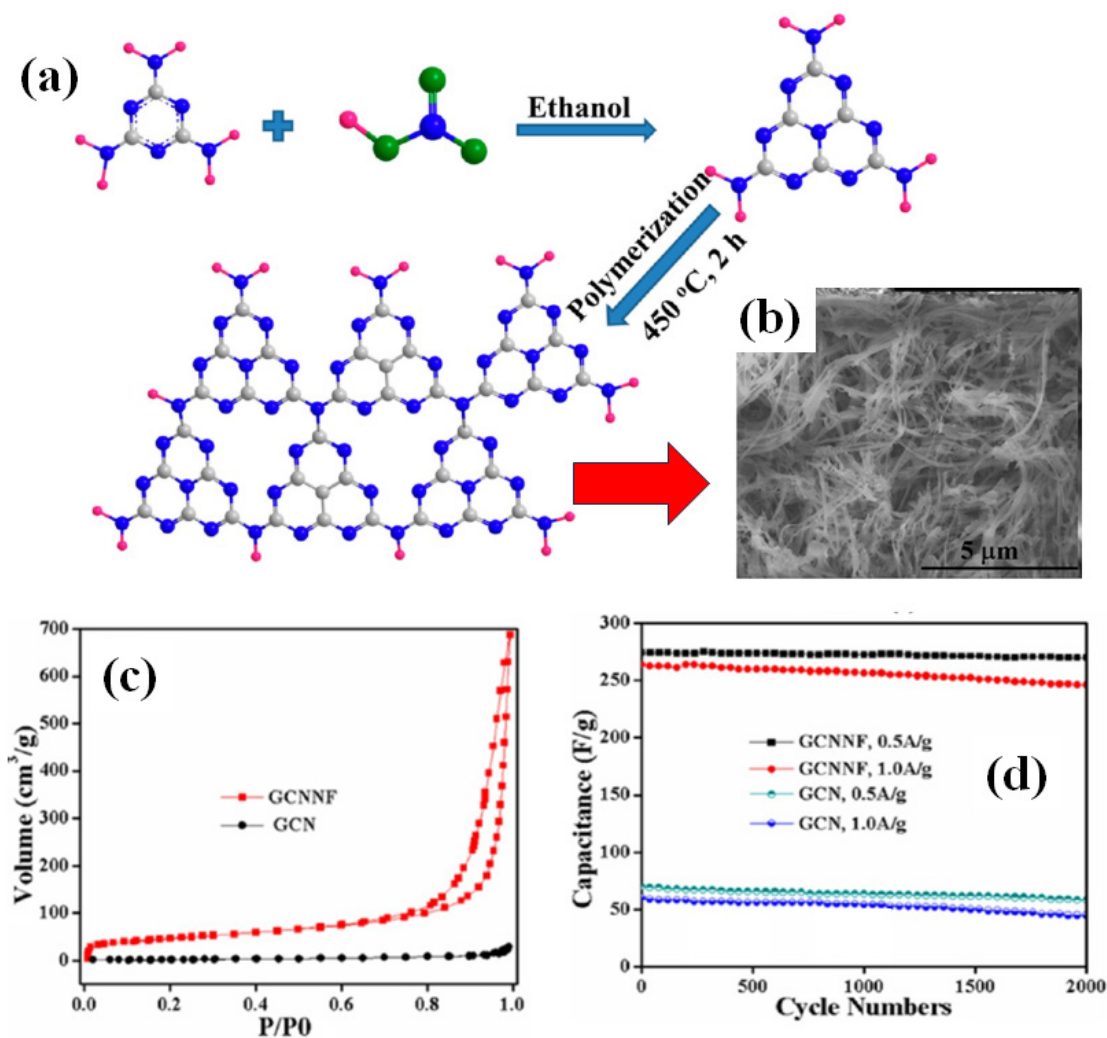


**Figure 5.** (a) Schematic presentation of green route synthesis of graphitic carbon nitride nanofiber and (b) its FESEM image; (c) Comparative dinitrogen adsorption-desorption isothermal curves for graphitic carbon nitride nanofiber and its bulk analogue; (d) Cyclic stability profiles for graphitic carbon nitride nanofiber and its bulk analogue<sup>[56]</sup>

In another work, the urge for designing high-performing all-solid-state supercapacitors encouraged the fabrication of flexible, ultrathin conductive graphitic carbon nitride sheets assembly that demonstrated ultrahigh areal energy density of  $281.3 \mu\text{Wh cm}^{-2}$  @ current density of  $1 \text{ mA cm}^{-2}$  with high-rate capacity

and coulombic efficiency<sup>[72]</sup>. Similarly, for the framing of high capacity all-solid supercaps, a unique film electrode mirroring Monstera leaf-like morphology was proposed that prompted construction of super-wettable electrodes for overcoming the sluggish ionic diffusion kinetics, and facilitated broad as well as easy ion-

accessible “highway” channels, for ultrafast diffusion of large sized ions of ionic gel electrolytes<sup>[73]</sup>. Lately, construction of highly-hydrophilic, poorly-crystalline and holey-ultrathin g-C<sub>3</sub>N<sub>4</sub> nanosheets have been very beneficial for providing excellent conducting matrix for designing various 3D heterostructured electroactive materials with magnificently improved electron transfer kinetics and capacitive signatures<sup>[74]</sup>.

Thus, it is very convincing that proper designing of morphology and adequate modification of synthetic methodology are very much essential steps needed to obtain the optimum quality of the graphitic carbon nitrides with superior electrochemical signatures.

### 4.3 Effect of Doping

Doping, as indicated from the relative performances of the g-C<sub>3</sub>N<sub>4</sub> systems reported in **Table 3**, has considerably influenced the properties of graphitic carbon nitride through: a) modification of the bandgap; b) enhancing adsorption capacity; c) modulation of the electronic structure; d) improved wettability and e) chemical reactivity<sup>[75-76]</sup>. Thus, Devi and coresearchers<sup>[62]</sup>, very recently, proposed a time saving and very effective synthetic approach to dope oxygen into the g-C<sub>3</sub>N<sub>4</sub> framework using H<sub>2</sub>O<sub>2</sub> in aid with microwave irradiation that modified the electronic states and surface structure to augment the capacitive aptitude as well as increased the wettability to facilitate better electrode-electrolyte interactions and faster ion transfer processes. The electrode system recorded much higher specific capacitance of 262.5 F g<sup>-1</sup> @ 1 A g<sup>-1</sup> current density, almost eight-fold augmented capacitive response compared to bulk g-C<sub>3</sub>N<sub>4</sub>, in addition to an acceptable capacitance retaining efficacy of 73.17% @ high current density of 6 A g<sup>-1</sup> even after 2000 charging/discharging cycles. The fabricated asymmetric supercapacitor using this material as a component recorded specific energy as high as 36.45 Wh kg<sup>-1</sup> @ specific power of 2.5 kW kg<sup>-1</sup><sup>[62]</sup>. Moreover, doping strategies involving cleavage of polymeric structures of g-C<sub>3</sub>N<sub>4</sub> subjected to strong oxidizing agents, resulted in the formation of higher density nitrogen-edged graphitic nitride that exhibit upgraded pseudocapacitance and improved conductivity<sup>[61]</sup>. Likewise, red-phosphorus doped graphitic carbon nitride heterostructures showed advanced capacitive outputs (465 F g<sup>-1</sup>) as well as appreciable capacitance

retention efficacy of 90% after undergoing continuous 1000 charging/ discharging cycles @ current of 10 A g<sup>-1</sup> attributed mainly to the modified band gap, enhanced surface area and cooperative capacitive contributions of both components in the hybrid system<sup>[63]</sup>. In another instance, sulphur doping in the graphitic carbon nitride has yielded higher capacitive values owing to the availability of greater number of sulphur and nitrogen-rich carbons offering abundant redox reactions sites for enhanced capacitive charge storage<sup>[77]</sup>.

Nonetheless, the progressive studies in this field pointed out the challenges faced during optimization of extent and concentrations of the doping process, thus, creating a non-climbable barrier from commercial aspect. Further, till date reported doping forms of graphitic carbon nitrides do not match with the commercial standards in terms of capacitance, life span, and energy densities due to inferior electrical conductivity, limited surface accessible area and spontaneous layer aggregation issues and thus further structural and functional modifications are recommended for their better workability in energy storage sector.

### 5. Supercapacitive Responses of Graphitic Carbon Nitride Composite Electrodes

Composite formation has always been a mutual benefitting process, simultaneously enhancing the capabilities of the associating components in a synergistic way when combined in appropriate proportions. Thus, to cope up with the existing issues of low energy storage and power delivering responses, graphitic carbon nitride has been subjected to nanocomposite formation through hybridization with various materials such as other nanocarbons, metallic oxides/ sulphides/ other chalcogenides or pnictides/carbides, metal derived systems, metal-organic framework or conducting polymer materials for better energy storage efficiency, as reflected from the data indicated in the **Table 4**. These materials have been schemed vide various fabrication approaches that include solvothermal, pyrolysis, chemical routes as well as multi-step techniques to introduce better morphological control which accordingly assists in tuning and tailoring the electrochemical signatures for advanced applications<sup>[78-113]</sup>.

**Table 4.** Some reported g-C<sub>3</sub>N<sub>4</sub> based nanocomposites for supercapacitor applications

| Materials  |  | N-precursor, synthesis process                | Electrolyte used                | Voltage window (V) | Specific capacitance (F g <sup>-1</sup> ) (current density in A g <sup>-1</sup> /voltage scan rate) | Cycle number | Capacitance retention (%) | Specific energy E (Wh kg <sup>-1</sup> ) | Specific power P (W kg <sup>-1</sup> ) | Ref. |
|--|--|---|---------------------------------|--------------------|---|--------------|---------------------------|--|--|------|
| Binary nanocomposites with nanocarbons           | rGO/carbon nitride   | Dicyandiamide, hydrothermal                   | KOH                             | -1.0-0.0           | 288 (0.5 A g <sup>-1</sup> )  | /            | /                         | 36.6                                     | 480                                    | [78] |
|  | g-C <sub>3</sub> N <sub>4</sub> /rGO   | Melamine, solvothermal method                 | KOH                             | -0.5-0.5           | 379.7 (0.25 A g <sup>-1</sup> )   | 10000        | 85                        | 52.7                                     | 500                                    | [79] |
|  | g-C <sub>3</sub> N <sub>4</sub> /nitrogen-enriched carbon spheres                      | Urea, thermal decomposition                   | /                               | -0.2-0.8           | 403.6 (0.1 A g <sup>-1</sup> )  | 5000         | 100                       | 6.75                                     | 1000                                   | [80] |
|  | g-C <sub>3</sub> N <sub>4</sub> /mesoporous carbon sphere                              | Melamine                                      | KOH                             | -0.2-0.6           | 352.44 (5 mV s <sup>-1</sup> )  | 3000         | 88.44                     | /  | /                                      | [81] |
|  | Carbon cloth/GCN   | Urea, glucose annealing                       | H <sub>2</sub> SO <sub>4</sub>  | 0.0-1.0            | 499 (1 A g <sup>-1</sup> )  | 10000        | 95.4                      | 10.1                                     | 10000                                  | [82] |
|  | g-C <sub>3</sub> N <sub>4</sub> assembly with graphene oxide                           | Urea, pyrolysis                               | H <sub>2</sub> SO <sub>4</sub>  | 0.0-0.8            | 936 mF cm <sup>-2</sup>   | 1000         | 100                       | 281.3 μWh cm <sup>-2</sup>               | 1.2 μW cm <sup>-2</sup>                | [83] |
| Binary nanocomposites with metal-based compounds | g-C <sub>3</sub> N <sub>4</sub> /Ni(OH) <sub>2</sub>                                   | Melamine, hydrothermal method                 | KOH                             | -0.1-0.5           | 505.6 (0.5 A g <sup>-1</sup> )  | 1000         | 71.5                      | 17.56                                    | 125.43                                 | [84] |
|  | g-C <sub>3</sub> N <sub>4</sub> /NiAl-LDH  | Urea, in situ self-assembly                   | KOH                             | -0.2-0.6           | 714 (0.5 A g <sup>-1</sup> )  | 10000        | 82                        | /  | /                                      | [85] |
|  | CNRG/Ni(OH) <sub>2</sub>   | hyper-acoustic-thermal treatment, oil bath    | KOH                             | 0.0-0.5            | 1785 (2 A g <sup>-1</sup> )   | 5000         | 71.3                      | /  | /                                      | [86] |
|  | Carbon-doped g-C <sub>3</sub> N <sub>4</sub> /MnO <sub>2</sub> (CCNM)                  | Melamine, hydrothermal method                 | Na <sub>2</sub> SO <sub>4</sub> | -0.2-0.8           | 324 (0.2 A g <sup>-1</sup> )  | 1000         | 80.2                      | /  | /                                      | [87] |
|  | K doped g-C <sub>3</sub> N <sub>4</sub> /MnO <sub>2</sub> (KCNM)                       | Thiourea, hydrothermal method                 | Na <sub>2</sub> SO <sub>4</sub> | -0.2-0.6           | 373.5 (0.2 A g <sup>-1</sup> )  | 1000         | 95.2                      | /  | /                                      | [88] |
|  | MnO <sub>2</sub> /g-C <sub>3</sub> N <sub>4</sub> NC                                   | Melamine, chemical route                      | Na <sub>2</sub> SO <sub>4</sub> | -0.2-0.8           | 211 (1 A g <sup>-1</sup> )  | 1000         | 100                       | /  | /                                      | [89] |
|  | Nanoneedle-assembled NiCo <sub>2</sub> O <sub>4</sub> /g-C <sub>3</sub> N <sub>4</sub> | thiourea, hydrothermal treatment, calcination | KOH                             | 0.0-0.6            | 274.8 (1 A g <sup>-1</sup> )  | 1000         | 89.4                      | /  | /                                      | [90] |
|  | Nanosheet assembled NiCo <sub>2</sub> O <sub>4</sub> /g-C <sub>3</sub> N <sub>4</sub>  | thiourea, oil bath treatment, calcination     | KOH                             | 0.0-0.6            | 118.2 (1 A g <sup>-1</sup> )  | 1000         | 101.4                     | /  | /                                      | [90] |
|  | g-C <sub>3</sub> N <sub>4</sub> /Ni(OH) <sub>2</sub> honeycomb structure               | Sonication, heat treatment                    | KOH                             | 0.0-0.5            | 1768.7 (7 A g <sup>-1</sup> )   | 8000         | 72                        | 43.1                                     | 9.126                                  | [91] |

Continuation Table:

| Materials  | N-precursor, synthesis process                      | Electrolyte used   | Voltage window (V)                     | Specific capacitance (F g <sup>-1</sup> ) (current density in A g <sup>-1</sup> /voltage scan rate) | Cycle number                 | Capacitance retention (%) | Specific energy E (Wh kg <sup>-1</sup> ) | Specific power P (W kg <sup>-1</sup> ) | Ref.    |       |
|--|---|--|--|---|------------------------------|---------------------------|--|--|---------|-------|
| g-C <sub>3</sub> N <sub>4</sub> /<br>α-Fe <sub>2</sub> O <sub>3</sub>          | Melamine, pyrolysis                                 | KOH  | 0.0-0.5                                | 580 (1 A g <sup>-1</sup> )  | 1000                         | 96                        | /  | /                                      | [92]    |       |
| Mesoporous Co <sub>3</sub> O <sub>4</sub> /<br>g-C <sub>3</sub> N <sub>4</sub> | Melamine, co-precipitation                          | KOH  | 0.0-0.5                                | 780 (1.25 A g <sup>-1</sup> )   | 1000                         | 80                        | /  | /                                      | [93]    |       |
| TiO <sub>2</sub> /g-C <sub>3</sub> N <sub>4</sub>                              | Dicyanamide, hydrothermal, heat Treatment           | KOH  | 0.0-0.5                                | 125.1 (1 A g <sup>-1</sup> )  | 1000                         | 100                       | /  | /                                      | [94]    |       |
| TiO <sub>2</sub> /g-C <sub>3</sub> N <sub>4</sub>                              | Thiourea, hydrothermal                              | KOH  | 0.0-1.0                                | 79.62 (1 A g <sup>-1</sup> )  | 9000                         | 92                        | /  | /                                      | [95]    |       |
| g-C <sub>3</sub> N <sub>4</sub> /<br>MnO <sub>2</sub>                          | Thiourea, oxidation-reduction reaction              | KOH  | 0.0-1.0                                | 174 (1 A g <sup>-1</sup> )  | 6000                         | 85                        | 24.1                                     | 1000                                   | [96]    |       |
| g-C <sub>3</sub> N <sub>4</sub> /<br>SnO <sub>2</sub>                          | Thiourea, chemical reduction method                 | KOH  | 0.0-1.0                                | 64 (1 A g <sup>-1</sup> )   | 6000                         | 87                        | 8.8                                      | 1000                                   | [96]    |       |
| Fe <sub>2</sub> O <sub>3</sub> nanospheres/<br>GCN                             | Melamine, hydrothermal                              | KOH  | 0.0-0.5                                | 243 (1 A g <sup>-1</sup> )  | 1000                         | 100                       | 70.22                                    | 800                                    | [97]    |       |
| NiCo <sub>2</sub> O <sub>4</sub> /<br>g-C <sub>3</sub> N <sub>4</sub>          | Melamine, in situ method                            | KOH  | 0.0-0.6                                | 1998 (2 A g <sup>-1</sup> )   | 5000                         | 95.2                      | /  | /                                      | [98]    |       |
| Self-repairing GCN/<br>NiCo <sub>2</sub> S <sub>4</sub>                        | Melamine, hydrothermal                              | KOH  | 0.0-0.6                                | 1557 (1 A g <sup>-1</sup> )   | 10000                        | 92.6                      | /  | /                                      | [99]    |       |
| Cobalt sulphide/<br>g-C <sub>3</sub> N <sub>4</sub>                            | Melamine, solvothermal                              | KOH  | -0.1-0.5                               | 834 (0.5 A g <sup>-1</sup> )  | 5000                         | 98                        | /  | /                                      | [100]   |       |
| SnS <sub>2</sub> -g-C <sub>3</sub> N <sub>4</sub>                              | Melamine, solvothermal                              | Na <sub>2</sub> SO <sub>4</sub>  | 0.0-0.5                                | 210.30 (0.5 A g <sup>-1</sup> )   | 1500                         | 84                        | /  | /                                      | [101]   |       |
| g-C <sub>3</sub> N <sub>4</sub> /<br>MoS <sub>2</sub>                          | Thiourea, sonication                                | Na <sub>2</sub> SO <sub>4</sub> -pva                                       | 0.0-0.4                                | 240.85 (1.0 A g <sup>-1</sup> )   | 100                          | 98                        | /  | /                                      | [102]   |       |
| MnS/g-C <sub>3</sub> N <sub>4</sub>  | Melamine, sol-gel                                   | Na <sub>2</sub> SO <sub>4</sub>  | -0.2-1.0                               | 573.9 (0.5 A g <sup>-1</sup> )  | 2000                         | 98.6                      | /  | /                                      | [103]   |       |
| Binary nanocomposites with conducting polymers                                 | PEDOT/<br>g-C <sub>3</sub> N <sub>4</sub>           | Melamine, layer-by-layer assembly  | H <sub>2</sub> SO <sub>4</sub>         | -0.2-0.8  | 137 (2 A g <sup>-1</sup> )   | 1000                      | 89                                       | 17.5                                   | 5000    | [104] |
|  | PEDOT/<br>g-C <sub>3</sub> N <sub>4</sub>           | Melamine, layer-by-layer assembly  | Na <sub>2</sub> SO <sub>4</sub>        | -0.6-0.6  | 200 (2 A g <sup>-1</sup> )   | 1000                      | 96.5                                     | 9.65                                   | 4001.86 | [104] |
|  | PANI/<br>g-C <sub>3</sub> N <sub>4</sub>            | Urea, oxidative polymerization   | H <sub>2</sub> SO <sub>4</sub>         | -0.2-1.2  | 584.3 (1 A g <sup>-1</sup> ) | 1000                      | 81.91                                    | /                                      | /       | [105] |
| Polypyrrole/<br>g-C <sub>3</sub> N <sub>4</sub>                                | Melamine, hydrothermal                              | KOH  | -1.0-0.2                               | 260.4 (1 A g <sup>-1</sup> )  | 2000                         | 80                        | /  | /                                      | [106]   |       |
| Ternary nanocomposite formation with g-C <sub>3</sub> N <sub>4</sub>           | PANI/<br>g-C <sub>3</sub> N <sub>4</sub> /<br>MXene | Melamine, in situ chemical polymerization and a vacuum-assisted filtration | PVA/H <sub>2</sub> SO <sub>4</sub> gel | -0.8-0.8  | 570 (5 mV s <sup>-1</sup> )  | 1000                      | 91.1                                     | 18.8                                   | 1563    | [107] |

| Materials  | N-precursor, synthesis process                     | Electrolyte used                | Voltage window (V) | Specific capacitance (F g <sup>-1</sup> ) (current density in A g <sup>-1</sup> /voltage scan rate) | Cycle number | Capacitance retention (%) | Specific energy E (Wh kg <sup>-1</sup> ) | Specific power P (W kg <sup>-1</sup> ) | Ref.  |
|--|--|---------------------------------|--------------------|---|--------------|---------------------------|--|--|-------|
| Surfactant immobilized mesoporous ternary polypyrrole /tubular g-C <sub>3</sub> N <sub>4</sub> @graphene | Melamine, polymerization followed by self-assembly | KOH                             | 0.0-0.5            | 260.4 (1 A g <sup>-1</sup> )  | 2000         | 80                        | /  | /                                      | [108] |
| Carbon/CuO nanosphere/ g-C <sub>3</sub> N <sub>4</sub>   | Thiourea, co pyrolysis decomposition               | NaOH                            | -0.6-0.6           | 247.2 (1 A g <sup>-1</sup> )  | 6000         | 92.1                      | /  | /                                      | [109] |
| RuO <sub>2</sub> / g-C <sub>3</sub> N <sub>4</sub> /rGO  | Melamine, hydrothermal & lyophilization            | KOH                             | -1.2-0.0           | 704.3 (0.5 A g <sup>-1</sup> )  | 2000         | 80.64                     | 2.60                                     | 223                                    | [110] |
| Ag/PANI/ g-C <sub>3</sub> N <sub>4</sub>   | Multi-step, in-situ oxidative polymerization.      | H <sub>2</sub> SO <sub>4</sub>  | 0.0-0.8            | 797.8 (0.1 A g <sup>-1</sup> )  | 1000         | 84.43                     | 14.44                                    | 5000                                   | [111] |
| FeV-WO <sub>3</sub> / g-C <sub>3</sub> N <sub>4</sub>  | Wet chemical approach                              | Na <sub>2</sub> SO <sub>4</sub> | -0.8-0.25          | 1033.68 (5 mV s <sup>-1</sup> )   | 2000         | 96.67                     | /  | /                                      | [112] |
| Ag-BiVO <sub>4</sub> / Bi <sub>2</sub> S <sub>3</sub> / g-C <sub>3</sub> N <sub>4</sub>                  | Wet chemical approach                              | KOH                             | 0.0-0.6            | 815.4 (1 A g <sup>-1</sup> )  | 5000         | 91.5                      | /  | /                                      | [113] |

Appropriate blending with various nanocarbons such as graphene, CNTs, fullerenes, have alleviated the resultant capacitance, by increasing the accessible surface area to the electrolyte ions as well as promoted the cycling stability resulting from suppression of unwanted aggregation effects synergistically attributed by each of the components in the resultant nanocomposites. Further, the versatile properties of various carbon materials in terms of structural and mechanical stability, extended pi-conjugation conferring superior conductivity and ease of material availability have driven scientists to synthesize nanocomposite with graphitic carbon nitride. Furthermore, in many cases, the similarity in electronic structures have been an additional advantage for nanocomposite formation with smoother interface, as in case of graphene and graphitic carbon nitride, for enhancing the supercapacitor performance relative to the bare components. For instance, g-C<sub>3</sub>N<sub>4</sub>@graphene composite exhibited an overall 75% increment in capacitance attributed to introduction of graphitic carbon nitride to graphene system owing to the reduced aggregation of graphene sheets thereby enhancing the

capacity retention efficacy during charging/discharging cyclic performances of the composite<sup>[60]</sup>.

Analogously, pristine pseudocapacitive conducting polymers such as polyaniline, polypyrroles, polythiophenes and their derivatives and metal-based compounds including oxides/ sulphides, metal derived systems, metal-organic framework *etc.*, irrespective of high theoretical capacitances, extremely suffer from poor rate capability, low cycling durability problems of the due to drastic structural degradations, easy detachment from the current collectors, electrolytic dissolution and side reactions. All these serious problems stand as mountain-high blockades in their marketable aspect. Thus, to address them successfully, they have been combined with graphitic carbon nitrides to form the nanocomposites that display enhanced electrochemical stabilities in both aqueous as well as in redox-active electrolytes relative to many other carbon-based composites already reported. Further, composite formation with g-C<sub>3</sub>N<sub>4</sub> have also resulted in dramatic rise in working voltage range of the resultant composites which have elevated the energy and power densities than till date observed. Accordingly, **Table 5** demonstrates some of the notable instances of



improvement of capacitive responses in the resultant nanocomposite, making them superior electroactive materials and simultaneously substantiating the important

role of g-C<sub>3</sub>N<sub>4</sub> as a very responsive electroactive component for framing smart and high-performing supercapacitive devices.

**Table 5.** Enhancement in electrochemical response for graphitic nanocomposite electrodes

| Electroactive g-C <sub>3</sub> N <sub>4</sub> based Materials   | Improvement in properties after nanocomposite formation            | Relative enhancement of electrochemical responses  | Ref.  |
|---|--|--|-------|
| Mesoporous GCN  | Nitrogen content   | Capacitance enhancement thrice-fold higher than bulk graphitic carbon nitride  | [60]  |
| Ni(OH) <sub>2</sub> /g-C <sub>3</sub> N <sub>4</sub>            | Morphology conversion (nanoplates to nanoflowers)                  | Nearly twice than bare-Ni (OH) <sub>2</sub> electrode  | [84]  |
| g-C <sub>3</sub> N <sub>4</sub> /NiAl-(LDH)                     | Surface area and pore size   | Capacitance enhancement 1.6-fold than pure LDH electrode and 25-fold than neat graphitic carbon nitride electrode  | [85]  |
| MnO <sub>2</sub> /g-C <sub>3</sub> N <sub>4</sub>               | Surface area   | Capacitance enhancement 2-fold than pristine MnO <sub>2</sub> electrode  | [89]  |
| g-C <sub>3</sub> N <sub>4</sub> /MnO <sub>2</sub>               | Surface area and pore size   | 2.6-fold higher than pristine MnO <sub>2</sub> electrode   | [96]  |
| GCN/Ni  | Surface area and pore size   | Nealy four times higher than bare-Ni(OH) <sub>2</sub> electrode  | [91]  |
| Co <sub>3</sub> O <sub>4</sub> /g-C <sub>3</sub> N <sub>4</sub> | Surface area and pore volume                                       | 1.8-fold higher than bare-Co <sub>3</sub> O <sub>4</sub> electrode   | [93]  |
| g-C <sub>3</sub> N <sub>4</sub> /SnO <sub>2</sub>               | Surface area and pore size   | 1.2-fold higher than pristine SnO <sub>2</sub> electrode   | [96]  |
| MoS <sub>2</sub> -g-C <sub>3</sub> N <sub>4</sub>               | High surface area, increased mass transfer                         | 5-fold higher than pristine MoS <sub>2</sub> electrode   | [102] |
| PEDOT/g-C <sub>3</sub> N <sub>4</sub>                           | High surface area, increased mass transfer                         | 1.1-fold higher than pristine PEDOT electrode  | [104] |
| PANI/g-C <sub>3</sub> N <sub>4</sub>                            | Good electron conductivity helped the fast electron transportation | 1.1 times greater than the pristine PANI electrode   | [105] |
| Ag/PANI/g-C <sub>3</sub> N <sub>4</sub> composite               | Enhancement in the cycling stability and electronic conductivity   | Improved and manifold rise in conductivity, specific capacitance and cyclic stability compared to bare-PANI and binary-PANI/g-C <sub>3</sub> N <sub>4</sub> electrodes | [111] |

Eventually, the high success rates with the varieties of binary nanocomposite electrodes have driven scientists in the designing of varieties of high performing ternary nanocomposite electrodes with the material which have finally displayed unique combination of the complementary properties of the components<sup>[107-113]</sup>. For example, very recently, a marked enhancement in electrochemical output in terms of enhanced charge storage behaviour, augmented rate capacity and distinct reduction in equivalent series resistance, as indicated in **Figure 6**, were observed while making a comparative study on the relative electrochemical responses between RuO<sub>2</sub>/graphene aerogel (RGA) binary nanocomposite and the ternary composite of RuO<sub>2</sub>/g-C<sub>3</sub>N<sub>4</sub>@graphene oxide aerogel (RCGA) respectively. The authors reported higher specific capacitances of 704.3 F g<sup>-1</sup> and 560.3 F g<sup>-1</sup> in the ternary and binary nanocomposite electrodes at the current density of 0.5 A g<sup>-1</sup> which was mainly attributed to the introduction of g-C<sub>3</sub>N<sub>4</sub> nanosheets that promoted larger surface area and availability of greater

number of reactive sites because of high nitrogen atom content leading to better pseudocapacitance in the resultant ternary nanocomposite<sup>[110]</sup>.

It is worthy to note that as far as structural assistances are concerned, the availability of non-bonded electron pairs on nitrogen in the g-C<sub>3</sub>N<sub>4</sub> have enhanced the surface polarity that stimulated the multiple binding process of electrolyte ions on the electrode surface. Thus, a substantial enhancement of wettability as well as smooth electron transfer in the carbon-g-C<sub>3</sub>N<sub>4</sub> based nanocomposite are frequently been observed. Moreover, distinct and periodic nitrogen based chemical structure have also provided numerous reactive nucleation sites towards formation of different nano-heterostructures with metal-based oxides, mixed oxides, sulphides, MXenes, *etc.* For instance, Ag-BiVO<sub>4</sub>/Bi<sub>2</sub>S<sub>3</sub> heterostructures grown on g-C<sub>3</sub>N<sub>4</sub> sheets through wet-chemical approach revealed outstanding capacitive responses owing to availability of ample redox active sites, increased wettability, as well as enhanced structural and chemical stabilities

relative to the Ag-BiVO<sub>4</sub>/Bi<sub>2</sub>S<sub>3</sub> electrode<sup>[112]</sup>. In several other strategies such as involving porous, ultrathin g-C<sub>3</sub>N<sub>4</sub> nanosheets uniformly decorated with NiCo<sub>2</sub>S<sub>4</sub> nanoparticles or be it iron/vanadium co-doped tungsten oxide nanostructures anchored on graphitic carbon nitride sheets, in each case, the superior heterostructure formation ensured effective heterojunctions formation that not only escalated the pseudocapacitance, but also

significantly reduced the agglomeration issues, along with creating suitable provision for enhancing the effective surface area to the electrolytic ions through enhanced availability of greater density of redox sites, shorter but wider ion-diffusion channels, significant enhancement of conductivity. All these inspiring results collectively prompted upgrading of the overall electrochemical performance in this system<sup>[90,113]</sup>.

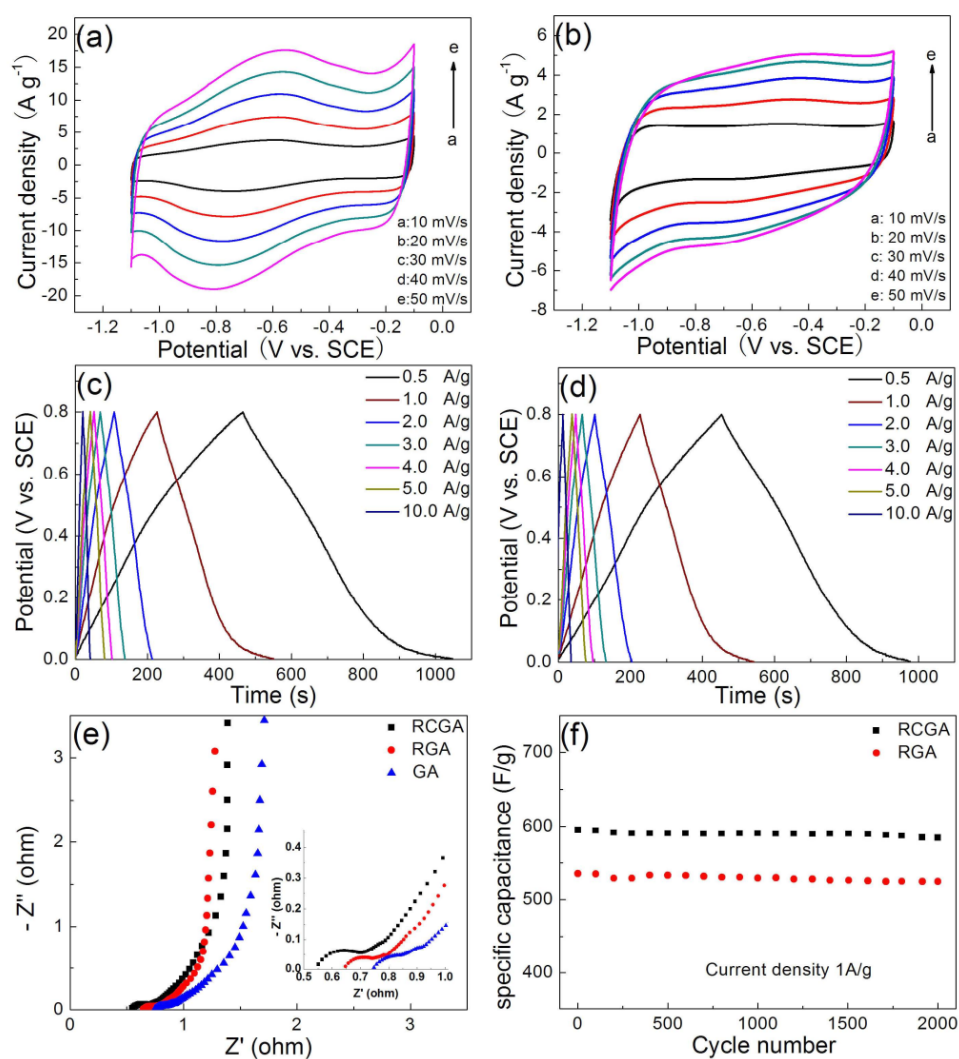


**Figure 6.** Cyclic voltammetric profiles of (a) ternary RuO<sub>2</sub>/g-C<sub>3</sub>N<sub>4</sub>@graphene oxide aerogel (RCGA) and (b) RuO<sub>2</sub>/graphene aerogel (RGA) binary composite electrodes at different scan rates, respectively; (c) and (d) Galvanostatic charging/discharging curves for curves ternary RuO<sub>2</sub>/g-C<sub>3</sub>N<sub>4</sub>@graphene oxide aerogel (RCGA) and RuO<sub>2</sub>/graphene aerogel (RGA) binary composite electrodes at different current densities, respectively; (e) Nyquist plots of ternary RuO<sub>2</sub>/g-C<sub>3</sub>N<sub>4</sub>@graphene oxide aerogel (RCGA) and RuO<sub>2</sub>/graphene aerogel (RGA) binary composite electrodes; (f) Cyclic stability of ternary RuO<sub>2</sub>/g-C<sub>3</sub>N<sub>4</sub>@graphene oxide aerogel (RCGA) and RuO<sub>2</sub>/graphene aerogel (RGA) binary composite electrodes respectively. Ref. [110], Preproduced on Copyright permission © 2017, American Chemical Society

As already stated, the need for self-powering wearable electronics have tremendously stimulated the growth of smart and proficient all-solid supercapacitors

in the recent days. The unique mechanical features of the carbon nitride have allowed formation of Ti<sub>3</sub>C<sub>2</sub>T<sub>x</sub>/g-C<sub>3</sub>N<sub>4</sub> hybrids which apart from admirable

energy densities, have successfully demonstrated their extreme capabilities to exhibit stable capacitive responses even under severe bending conditions<sup>[114]</sup>. Similarly, the essentiality of designing smart, flexible and auto-powering device for different biomedical applications have triggered fabrication of facile, bio-compatible all-solid-state supercapacitors using g-C<sub>3</sub>N<sub>4</sub> nanowires and polyvinyl alcohol and poly(3,4 ethylenedioxythiophene)/ poly(styrenesulfonate) hybrid electrode material with appreciable results<sup>[115]</sup>.

Needless to mention that the research on graphitic carbon nitride-based supercapacitor systems is in a very nascent stage but its investigations in this technological field have been accelerating at a high pace in these recent years. The main cause is attributed to the many of the experiential results obtained till date that have motivated the idea for more systematic analysis for developing smarter and flexible electrochemical energy storage systems in the near future<sup>[116]</sup>. Apart from the enhancement in electrochemical stability and cyclic performances, the energy and power density values have been exhibiting elevating responses for these electrode systems. The Ragone plot, as depicted from the **Figure 7**, clearly demonstrates the prominent improvement of energy responses starting from pristine

forms to g-C<sub>3</sub>N<sub>4</sub> binary nanocomposites and then to the corresponding ternary hybrids, (as depicted from the data in **Table 3** and **Table 4**) all targeting to achieve somewhere in the upper right positions in the Ragone plot. Besides, the observed capacitive performances in numerous occasions, have been found impressive compared to many of the popular, meticulously designed high-performing nanocarbon-based nanocomposites reported in the literature<sup>[117,118]</sup>. These preliminary findings have clearly driven worldwide scientists to search for the determining factors in terms of synthetic methodology, composition, carbon-nitrogen ratio, morphology, heterostructure formation, *etc.*, which can trigger superior electrochemical responses with these carbon nitride materials. It is obvious that the more progressive varieties of binary, ternary and polynary nanocomposites with advanced heterojunctions using simple, cost-effective fabrication strategies are highly recommended. Thus, it is evident that this promising material with advanced structural and electrochemical features have paved new prospects and networks towards designing more efficient and high performing electrochemical energy storage devices in the near future.

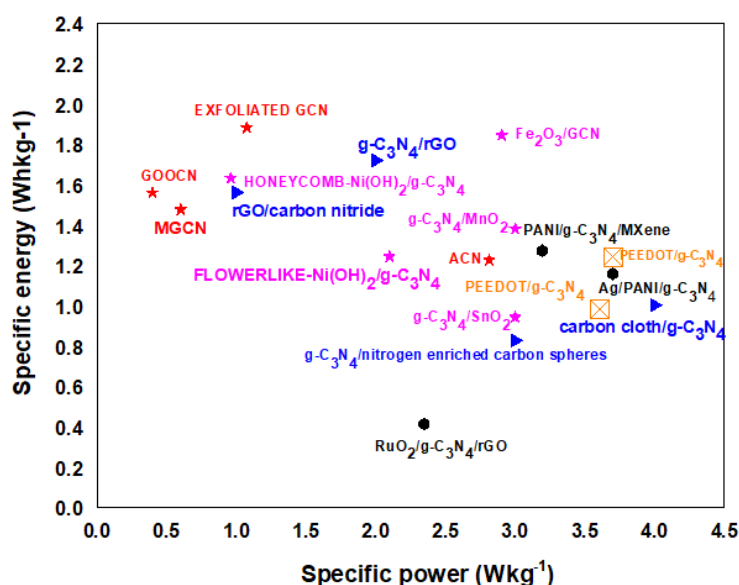


**Figure 7.** Ragone plot comparing the relative performances of various types of g-C<sub>3</sub>N<sub>4</sub> (GCN) system as depicted from the data in **Table 3** and **Table 4**, including different GCN nanostructures (indicated by red-coloured points) and some of its different binary (nanocarbon based -graphitic carbon nitride nanocomposites are indicated by blue-coloured points, conducting polymer based nanocomposites are indicated by orange-coloured points while the metal-based graphitic carbon nitride nanocomposites are indicated by pink-coloured points respectively) and ternary (indicated by back-coloured points) nanocomposites employed for supercapacitor applications

## 6. Concluding Remarks and Future Prospects

The above studies thus clearly reveal that g-C<sub>3</sub>N<sub>4</sub> based materials possess very promising applications in energy conversion and storage technologies. Nonetheless, the current research is at its very nascent stage and a number of concerns are to be immediately taken care of for its rapid and fruitful commercialization.

**Controlled synthesis to yield homogeneous, continuous, atomic-thick g-C<sub>3</sub>N<sub>4</sub> layers.** Fabrication of high-quality g-C<sub>3</sub>N<sub>4</sub> by optimizing the reaction conditions of fabrication techniques as well as through variation of the precursors, deposition temperature, *etc.* are yet to be pursued. Further, bulk g-C<sub>3</sub>N<sub>4</sub> materials obtained via simple techniques often involve severe post-synthesis treatments via exfoliation and etching processes, *etc.*, which should be tuned for better surface properties, reproducibility, yield and electrochemical efficiency.

**Improvement of conductivity.** At present, the pristine g-C<sub>3</sub>N<sub>4</sub> material exhibit poor conductivity due to irresistible layer stacking that remains as the major barrier in their practicability. To cope up with the issue, various morphologies such as nanorods, spheres, 2D layers, nanosheets, *etc.* of g-C<sub>3</sub>N<sub>4</sub> materials have been opted to enable better electron transfer kinetics. Further doping with heteroatoms such as oxygen, boron, phosphorus, *etc.* have also exhibited better adaptability towards tuneable electronic and surface properties. Nonetheless, nature and amount of doping level has to be optimized for observing utmost energy storage performances.

**Rational design of complex heterostructures.** Nano-heterostructured composites possessing well-designed architectures obtainable via judicious designing and composition have to be targeted using feasible approach via green and cost-effective strategy synthesis.

**Fundamental understanding of the charge transport process in these nanocomposites.** More exhaustive and organized studies will promote better and critical understanding of the charge generation, storage and transportation processes, which are critical for understanding the charge generation, separation and transportation across these nanoscale interfaces within the electrode material as well as at the electrolyte interfaces. Such detailed mechanistic studies of the charge transfer exercise integrating two, three or even

more components would assist in delineating the necessary conditions for optimum electrode / device performances in the near future.

**Appropriate combinations of the components in forming smart nanocomposites.** Further, it has been noticed that the majority of the carbonaceous nanocomposites deliver better specific power owing to their high charge transport kinetics in comparison to the metallic or conducting polymer binary nanocomposites. The latter, on the contrary, owing to their enhanced cumulative pseudocapacitive responses hikes the specific energies considerably compared to the former cases. Therefore, the appropriate combinations of components and optimization of composition in binary, ternary or polynary nanocomposites are important for rendering better charge storage as well as delivering capacity.

**Studies relating to eco-compatibility and stability of these nanocomposites.** Further, detailed studies relating to thermal, electrochemical and mechanical stabilities of g-C<sub>3</sub>N<sub>4</sub>-based nanocomposites have been less explored. Besides, while framing wearable electronics, eco-compatibility is a big factor that needs immediate examinations and stands as one of the major challenges in fabricating flexible self-powered electronics to be practically utilized in stringent environments, particularly in the domains of defence, astronomical and biomedical applications.

**Multifunctional applications of these nanocomposites.** Besides charge storage, other elaborative scientific explorations must be made to explore and understand the different properties of the materials which can be simultaneously clubbed together and used in the designing of multi-functional self-powered gadgets to improve their technological applications.

Thus, it is well perceived that with the rapid development of material science and nanotechnology and combined efforts of scientists worldwide such creation and development of advanced properties in these materials would be very interesting and accomplishable indeed. Such industrious endeavour will obviously help in resolving the highly critical environmental and energy-related global issues in the near future.

## Acknowledgements

Majumdar D acknowledges Chandernagore College, Chandannagar, Hooghly, West Bengal, Pin-712136, India, for providing permission to do honorary research. Majumdar D also acknowledges all well-wishers for constant encouragement for carrying out research activities. Sarkar R and Mondal M acknowledge their affiliating institutes, IIT Dhanbad and IIT Kharagpur, respectively, for the academic and research supporting facilities.

## Author's Contributions

Collection of data, writing-original draft: Sarkar R, Mondal M

Conceptualization, supervision, validation, visualization, writing-review and editing: Majumdar D

## Ethics Statement

Not applicable.

## Consent for publication

Not applicable.

## Availability of Supporting Data

Not applicable.

## Conflict of Interest

The author declares no conflict of interest and no fund assistance received from any sources or any organization for the present project.

## Copyright

© The Author(s) 2023.

## References

- [1] Abdel Maksoud MIA, Fahim RA, Shalan AE, *et al.* Advanced materials and technologies for supercapacitors used in energy conversion and storage: a review. *Environmental Chemistry Letters*, 2021;19:375-439.  
<https://doi.org/10.1007/s10311-020-01075-w>
- [2] Zhang H, Zhang J, Gao X, *et al.* Advances in materials and structures of supercapacitors. *Ionics*, 2022;28:515-531.  
<https://doi.org/10.1007/s11581-021-04359-5>
- [3] Simon P, Gogotsi Y and Dunn B. Where do batteries end and supercapacitors begin?. *Science*, 2014;343(6176):1210-1211.  
<https://doi.org/10.1126/science.1249625>
- [4] Aderyani S, Flouda P, Shah SA, *et al.* Simulation of cyclic voltammetry in structural supercapacitors with pseudocapacitance behavior. *Electrochimica Acta*, 2021;390:138822.  
<https://doi.org/10.1016/j.electacta.2021.138822>
- [5] Kumar N, Kim SB, Lee SY, *et al.* Recent advanced supercapacitor: a review of storage mechanisms, electrode materials, modification, and perspectives. *Nanomaterials*, 2022;12(20):3708.  
<https://doi.org/10.3390/nano12203708>
- [6] Şahin ME, Blaabjerg F and Sangwongwanich A. A comprehensive review on supercapacitor applications and developments. *Energies*, 2022;15(3):674.  
<https://doi.org/10.3390/en15030674>
- [7] Zhao Z, Xia K, Hou Y, *et al.* Designing flexible, smart and self-sustainable supercapacitors for portable/wearable electronics: from conductive polymers. *Chemical Society Reviews*, 2021;50(22):12702-12743.  
<https://doi.org/10.1039/D1CS00800E>
- [8] Islam MR, Afroj S, Novoselov KS, *et al.* Smart electronic textile-based wearable supercapacitors. *Advanced Science*, 2022;9(31):2203856.  
<https://doi.org/10.1002/advs.202203856>
- [9] Qu X, Kwon YW, Jeon S, *et al.* Foldable and wearable supercapacitors for powering healthcare monitoring applications with improved performance based on hierarchically co-assembled CoO/NiCo networks. *Journal of Colloid and Interface Science*, 2023;634:715-729.  
<https://doi.org/10.1016/j.jcis.2022.12.005>
- [10] Ansari SA, Ansari MO and Cho MH. Facile and scale up synthesis of red phosphorus-graphitic carbon nitride heterostructures for energy and environment applications. *Scientific Reports*, 2016;6(1):27713.  
<https://doi.org/10.1038/srep27713>
- [11] Yaseen M, Khattak MAK, Humayun M, *et al.* A review of supercapacitors: materials design, modification, and applications. *Energies*, 2021;14(22):7779.  
<https://doi.org/10.3390/en14227779>
- [12] Muzaffar A, Ahamed MB, Deshmukh K, *et al.* A review on recent advances in hybrid

- supercapacitors: design, fabrication and applications. *Renewable and Sustainable Energy Reviews*, 2019;101:123-145.  
<https://doi.org/10.1016/j.rser.2018.10.026>
- [13] Majumdar D and Ghosh S. Recent advancements of copper oxide based nanomaterials for supercapacitor applications. *Journal of Energy Storage*, 2021;34:101995.  
<https://doi.org/10.1016/j.est.2020.101995>
- [14] Majumdar D. Recent progress in copper sulfide based nanomaterials for high energy supercapacitor applications. *Journal of Electroanalytical Chemistry*, 2021;880:114825.  
<https://doi.org/10.1016/j.jelechem.2020.114825>
- [15] Majumdar D and Das HT. Liquid electrolytes for supercapacitors. In: Gupta R (Eds). *Handbook of Energy Materials*: Springer, Singapore; 2022.  
[https://doi.org/10.1007/978-981-16-4480-1\\_22-1](https://doi.org/10.1007/978-981-16-4480-1_22-1)
- [16] Majumdar D and Bhattacharya SK. Polymer electrolytes for supercapacitor applications. In: Inamuddin Ahamed MI, Boddula R, Altalhi TA (Eds). *Polymers in Energy Conversion and Storage* (1<sup>st</sup> Ed). CRC Press; 2022.  
<https://doi.org/10.1201/9781003169727>
- [17] Majumdar D. Review on current progress of MnO<sub>2</sub>-based ternary nanocomposites for supercapacitor applications. *ChemElectroChem*, 2021;8(2):291-336.  
<https://doi.org/10.1002/celec.202001371>
- [18] Majumdar D. Aqueous electrolytes for flexible supercapacitors: In Flexible Supercapacitor Nanoarchitectonics. In: Inamuddin Ahamed MI, Boddula R, Altalhi TA (Eds); 2021.  
<https://doi.org/10.1002/9781119711469.ch13>
- [19] Khan IA, Thekkekara L, Waqar S, *et al.* Supercapacitors fabrication and performance evaluation techniques. IntechOpen. 2022.  
<https://doi.org/10.5772/intechopen.101748>
- [20] Sharma S and Chand P. Supercapacitor and electrochemical techniques: a brief review. *Results in Chemistry*, 2023;5:100885.  
<https://doi.org/10.1016/j.rechem.2023.100885>
- [21] Majumdar D, Maiyalagan T and Jiang Z. Recent progress in ruthenium oxide-based composites for supercapacitor applications. *ChemElectroChem*, 2019;6(17):4343-4372.  
<https://doi.org/10.1002/celec.201900668>
- [22] Majumdar D. Polyaniline as proficient electrode material for supercapacitor applications: PANI nanocomposites for supercapacitor applications. In: Ramdani N (editors). *Polymer Nanocomposites for Advanced Engineering and Military Applications*. IGI Global; 2019. p. 190-219.  
<https://doi.org/10.4018/978-1-5225-7838-3.ch007>
- [23] Das K and Majumdar D. Prospects of MXenes/graphene nanocomposites for advanced supercapacitor applications. *Journal of Electroanalytical Chemistry*, 2022;905:115973.  
<https://doi.org/10.1016/j.jelechem.2021.115973>
- [24] Majumdar D. Role of MXenes/polyaniline nanocomposites in fabricating innovative supercapacitor technology. *Advanced Energy Conversion Materials*, 2022;3(1):30-53.  
<https://doi.org/10.37256/aecm.3120221148>
- [25] Majumdar D, Mandal M and Bhattacharya SK. Journey from supercapacitors to supercapatteries: recent advancements in electrochemical energy storage systems. *Emergent Materials*, 2020;3:347-367.  
<https://doi.org/10.1007/s42247-020-00090-5>
- [26] Chaudhary K, Basha B, Zulfiqar S, *et al.* 3D cellular lattice like-Ti<sub>3</sub>C<sub>2</sub> MXene based aerogels embedded with metal selenides particles for energy storage and water splitting applications. *Fuel*, 2023;351:128856.  
<https://doi.org/10.1016/j.fuel.2023.128856>
- [27] Iro Z S, Subramani C, Dash S S. A brief review on electrode materials for supercapacitor. *International Journal of Electrochemical Science*, 2016;11(12):10628-10643.  
<https://doi.org/10.20964/2016.12.50>
- [28] Benoy SM, Pandey M, Bhattacharjya D, *et al.* Recent trends in supercapacitor-battery hybrid energy storage devices based on carbon materials. *Journal of Energy Storage*, 2022;52:104938.  
<https://doi.org/10.1016/j.est.2022.104938>
- [29] Wang Y and Xia Y. Recent progress in supercapacitors: from materials design to system construction. *Advanced Materials*, 2013;25(37):5336-5342.  
<https://doi.org/10.1002/adma.201301932>
- [30] Yang W, Ni M, Ren X, *et al.* Graphene in supercapacitor applications. *Current Opinion in Colloid & Interface Science*, 2015;20(5-6):416-

428.  
<https://doi.org/10.1016/j.cocis.2015.10.009>
- [31] Majumdar D. Application of microbes in synthesis of electrode materials for supercapacitors: application of microbes in environmental and microbial biotechnology. In: Inamuddin Ahamed MI, Prasad R (Eds). *Environmental and Microbial Biotechnology*. Singapore: Springer; 2022.  
[https://doi.org/10.1007/978-981-16-2225-0\\_2](https://doi.org/10.1007/978-981-16-2225-0_2)
- [32] Kumar P, Abuhimad H, Wahyudi W, *et al.* Review-two-dimensional layered materials for energy storage applications. *ECS Journal of Solid State Science and Technology*, 2016;5:Q3021-Q3025.  
<https://doi.org/10.1149/2.0051611jss>
- [33] Hasan MAM, Wang Y, Bowen CR, *et al.* 2D nanomaterials for effective energy scavenging. *Nano-Micro Letters*, 2021;13:82.  
<https://doi.org/10.1007/s40820-021-00603-9>
- [34] Zhai Z, Zhang L, Du T, *et al.* A review of carbon materials for supercapacitors. *Materials & Design*, 2022;221:111017.  
<https://doi.org/10.1016/j.matdes.2022.111017>
- [35] Majumdar D. Ultrasound-assisted synthesis, exfoliation and functionalisation of graphene derivatives. In: Khan A, Jawaid M, Neppolian B, Asiri A (Eds). *Graphene Functionalization Strategies. Carbon Nanostructures*. Singapore: Springer; 2019.  
[https://doi.org/10.1007/978-981-32-9057-0\\_3](https://doi.org/10.1007/978-981-32-9057-0_3)
- [36] Velasco A, Ryu YK, Boscá A, *et al.* Recent trends in graphene supercapacitors: from large area to microsupercapacitors. *Sustainable Energy & Fuels*, 2021;5(5):1235-1254.  
<https://doi.org/10.1039/D0SE01849J>
- [37] Chaudhary K, Zulfiqar S, Somaily HH, *et al.* Rationally designed multifunctional  $Ti_3C_2$  MXene@ Graphene composite aerogel integrated with bimetallic selenides for enhanced supercapacitor performance and overall water splitting. *Electrochimica Acta*, 2022;431:141103.  
<https://doi.org/10.1016/j.electacta.2022.141103>
- [38] Anwar M, Cochran EW, Zulfiqar S, *et al.* In-situ fabricated copper-holmium co-doped cobalt ferrite nanocomposite with cross-linked graphene as novel electrode material for supercapacitor application. *Journal of Energy Storage*, 2023;72:108438.  
<https://doi.org/10.1016/j.est.2023.108438>
- [39] Yan X, You H, Liu W, *et al.* Free-standing and heteroatoms-doped carbon nanofiber networks as a binder-free flexible electrode for high-performance supercapacitors. *Nanomaterials*, 2019;9(9):1189.  
<https://doi.org/10.3390/nano9091189>
- [40] Zhu J, Xiao P, Li H, *et al.* Graphitic carbon nitride: synthesis, properties, and applications in catalysis. *ACS Applied Materials & Interfaces*, 2014;6(19):16449-16465.  
<https://doi.org/10.1021/am502925j>
- [41] Lee WJ, Maiti UN, Lee JM, *et al.* Nitrogen-doped carbon nanotubes and graphene composite structures for energy and catalytic applications. *Chemical Communications*, 2014;50(52):6818-6830.  
<https://doi.org/10.1039/C4CC00146J>
- [42] Wang J and Wang S. A critical review on graphitic carbon nitride (g- $C_3N_4$ )-based materials: preparation, modification and environmental application. *Coordination Chemistry Reviews*, 2022;453:214338.  
<https://doi.org/10.1016/j.ccr.2021.214338>
- [43] Yang G, Li L, Lee WB, *et al.* Structure of graphene and its disorders: a review. *Science and Technology of Advanced Materials*, 2018;19(1):613-648.  
<https://doi.org/10.1080/14686996.2018.1494493>
- [44] Xu X, Liu C, Sun Z, *et al.* Interfacial engineering in graphene bandgap. *Chemical Society Reviews*, 2018;47(9):3059-3099.  
<https://doi.org/10.1039/C7CS00836H>
- [45] Ke Q and Wang J. Graphene-based materials for supercapacitor electrodes-a review. *Journal of Materiomics*, 2016;2(1):37-54.  
<https://doi.org/10.1016/j.jmat.2016.01.001>
- [46] Olatunde OC and Onwudiwe DC. A comparative study of the effect of graphene oxide, graphitic carbon nitride, and their composite on the photocatalytic activity of  $Cu_3SnS_4$ . *Catalysts*, 2022;12(1):14.  
<https://doi.org/10.3390/catal12010014>
- [47] Ghaemmaghami M and Mohammadi R. Carbon nitride as a new way to facilitate the next generation of carbon-based supercapacitors. *Sustainable Energy & Fuels*, 2019;3(9):2176-2204.  
<https://doi.org/10.1039/C9SE00313D>

- [48] Sekhar MC, Kumar NS, Asif M, *et al.* Enhancing electrochemical performance with g-C<sub>3</sub>N<sub>4</sub>/CeO<sub>2</sub> binary electrode material. *Molecules*, 2023;28(6):2489.  
<https://doi.org/10.3390/molecules28062489>
- [49] Ashritha MG and Hareesh K. A review on graphitic carbon nitride based binary nanocomposites as supercapacitors. *Journal of Energy Storage*, 2020;32:101840.  
<https://doi.org/10.1016/j.est.2020.101840>
- [50] Chahkandi M, Zargazi M, Ahmadi A, *et al.* In situ synthesis of holey g-C<sub>3</sub>N<sub>4</sub> nanosheets decorated by hydroxyapatite nanospheres as efficient visible light photocatalyst. *RSC Advances*, 2021;11(50):31174-31188.  
<https://doi.org/10.1039/D1RA05259D>
- [51] Chen X, Wang X, Liu F, *et al.* Fabrication of NiO-ZnO-modified g-C<sub>3</sub>N<sub>4</sub> hierarchical composites for high-performance supercapacitors. *Vacuum*, 2020;178:109453.  
<https://doi.org/10.1016/j.vacuum.2020.109453>
- [52] Nayak D, Mandal G, Kumar S, *et al.* Scalable one-step template-free synthesis of ultralight edge-multifunctionalized g-C<sub>3</sub>N<sub>4</sub> nanosheets with enhanced optical and electrochemical properties. In: Khan ZH, Jackson M, Salah NA (eds). *Recent Advances in Nanomaterials*. ICNOC 2022. Springer Proceedings in Materials. Singapore: Springer. 2022. p. 281-286.  
[https://doi.org/10.1007/978-981-99-4878-9\\_39](https://doi.org/10.1007/978-981-99-4878-9_39)
- [53] Thiagarajan K, Bavani T, Arunachalam P, *et al.* Nanofiber NiMoO<sub>4</sub>/g-C<sub>3</sub>N<sub>4</sub> composite electrode materials for redox supercapacitor applications. *Nanomaterials*, 2020;10(2):392.  
<https://doi.org/10.3390/nano10020392>
- [54] Nabi G, Riaz KN, Nazir M, *et al.* Cogent synergic effect of TiS<sub>2</sub>/g-C<sub>3</sub>N<sub>4</sub> composite with enhanced electrochemical performance for supercapacitor. *Ceramics International*, 2020;46(17):27601-27607.  
<https://doi.org/10.1016/j.ceramint.2020.07.254>
- [55] Wang A, Wang C, Fu L, *et al.* Recent advances of graphitic carbon nitride-based structures and applications in catalyst, sensing, imaging, and LEDs. *Nano-Micro Letters*, 2017;9:47.  
<https://doi.org/10.1007/s40820-017-0148-2>
- [56] Tahir M, Cao C, Mahmood N, *et al.* Multifunctional g-C<sub>3</sub>N<sub>4</sub> nanofibers: a template-free fabrication and enhanced optical, electrochemical, and photocatalyst properties. *ACS Applied Materials & Interfaces*, 2014;6(2):1258-1265.  
<https://doi.org/10.1021/am405076b>
- [57] Tahir M, Cao C, Butt FK, *et al.* Tubular graphitic-C<sub>3</sub>N<sub>4</sub>: a prospective material for energy storage and green photocatalysis. *Journal of Materials Chemistry A*, 2013;1(44):13949-13955.  
<https://doi.org/10.1039/C3TA13291A>
- [58] Shen C, Li R, Yan L, *et al.* Rational design of activated carbon nitride materials for symmetric supercapacitor applications. *Applied Surface Science*, 2018;455:841-848.  
<https://doi.org/10.1016/j.apsusc.2018.06.065>
- [59] Gonçalves R, Lima TM, Paixão MW, *et al.* Pristine carbon nitride as active material for high-performance metal-free supercapacitors: simple, easy and cheap. *RSC Advances*, 2018;8(61):35327-35336.  
<https://doi.org/10.1039/c8ra06656f>
- [60] Hao W and Teng F. Molten-state cubic cage-templated uniform C<sub>3</sub>N<sub>4</sub> hollow nanocubes and improved electrochemical performance of asymmetric micro-supercapacitor. *Journal of Alloys and Compounds*, 2022;909:164790.  
<https://doi.org/10.1016/j.jallcom.2022.164790>
- [61] Lin R, Li Z, Abou El Amaiem DI, *et al.* A general method for boosting the supercapacitor performance of graphitic carbon nitride/graphene hybrids. *Journal of Materials Chemistry A*, 2017;5(48):25545-25554.  
<https://doi.org/10.1039/c7ta09492b>
- [62] Devi M, Yesmin S, Das B, *et al.* Efficient oxygen doping of graphitic carbon nitride by green microwave irradiation for high-performance supercapacitor electrode material. *Energy & Fuels*, 2023;37(4):3247-3259.  
<https://doi.org/10.1021/acs.energyfuels.2c04083>
- [63] Ma D, Li X, Wang X, *et al.* Research development on graphitic carbon nitride and enhanced catalytic activity on ammonium perchlorate. *RSC Advances*, 2021;11(10):5729-5740.  
<https://doi.org/10.1039/D0RA09079D>
- [64] Wehrstedt KD, Wildner W, Gütthner T, *et al.* Safe transport of cyanamide. *Journal of Hazardous Materials*, 2009;170(2-3):829-835.  
<https://doi.org/10.1016/j.jhazmat.2009.05.043>



- [65] Xu J, Wu HT, Wang X, *et al.* A new and environmentally benign precursor for the synthesis of mesoporous g-C<sub>3</sub>N<sub>4</sub> with tunable surface area. *Physical Chemistry Chemical Physics*, 2013; 15(13):4510-4517.  
<https://doi.org/10.1039/C3CP44402C>
- [66] Wang S, Li Y, Wang X, *et al.* One-step supramolecular preorganization constructed crinkly graphitic carbon nitride nanosheets with enhanced photocatalytic activity. *Journal of Materials Science & Technology*, 2022;104:155-162.  
<https://doi.org/10.1016/j.jmst.2021.07.014>
- [67] Wang D, Wang Y, Chen Y, *et al.* Coal tar pitch derived N-doped porous carbon nanosheets by the in-situ formed g-C<sub>3</sub>N<sub>4</sub> as a template for supercapacitor electrodes. *Electrochimica Acta*, 2018;283:132-140.  
<https://doi.org/10.1016/j.electacta.2018.06.151>
- [68] Idris MB and Sappani D. Unveiling mesoporous graphitic carbon nitride as a high performance electrode material for supercapacitors. *Chemistry Select*, 2018;3(40):11258-11269.  
<https://doi.org/10.1002/slct.201801752>
- [69] Idris MB and Devaraj S. Tuning the chemical composition, textural and capacitance properties of mesoporous graphitic carbon nitride. *Electrochimica Acta*, 2019;303:219-230.  
<https://doi.org/10.1016/j.electacta.2019.02.081>
- [70] Ghanem LG, Hamza MA, Taha MM, *et al.* Symmetric supercapacitor devices based on pristine g-C<sub>3</sub>N<sub>4</sub> mesoporous nanosheets with exceptional stability and wide operating voltage window. *Journal of Energy Storage*, 2022;52:104850.  
<https://doi.org/10.1016/j.est.2022.104850>
- [71] Liang Q, Ye L, Xu Q, *et al.* Graphitic carbon nitride nanosheet-assisted preparation of N-enriched mesoporous carbon nanofibers with improved capacitive performance. *Carbon*, 2015; 94:342-348.  
<https://doi.org/10.1016/j.carbon.2015.07.001>
- [72] Lu C, Yang Y and Chen X. Ultra-thin conductive graphitic carbon nitride assembly through van der waals epitaxy toward high-energy-density flexible supercapacitors. *Nano Letters*, 2019;19(6):4103-4111.  
<https://doi.org/10.1021/acs.nanolett.9b01511>
- [73] Shi M, Yang C, Yan C, *et al.* Boosting ion dynamics through superwettable leaf-like film based on porous g-C<sub>3</sub>N<sub>4</sub> nanosheets for ionogel supercapacitors. *NPG Asia Materials*, 2019;11(1):61.  
<https://doi.org/10.1038/s41427-019-0161-7>
- [74] Paliwal MK and Meher SK. 3D-heterostructured NiO nanofibers/ultrathin g-C<sub>3</sub>N<sub>4</sub> holey nanosheets: an advanced electrode material for all-solid-state asymmetric supercapacitors with multi-fold enhanced energy density. *Electrochimica Acta*, 2020;358:136871.  
<https://doi.org/10.1016/j.electacta.2020.136871>
- [75] Wang J and Han WQ. A review of heteroatom doped materials for advanced lithium-sulfur batteries. *Advanced Functional Materials*, 2022;32(2):2107166.  
<https://doi.org/10.1002/adfm.202107166>
- [76] Cui C, Gao Y, Li J, *et al.* Origins of boosted charge storage on heteroatom-doped carbons. *Angewandte Chemie*, 2020;132(20):8002-8007.  
<https://doi.org/10.1002/anie.202000319>
- [77] Ma JS, Yang H, Kubendhiran S, *et al.* Novel synthesis of sulfur-doped graphitic carbon nitride and NiCo<sub>2</sub>S<sub>4</sub> composites as efficient active materials for supercapacitors. *Journal of Alloys and Compounds*, 2022;903:163972.  
<https://doi.org/10.1016/j.jallcom.2022.163972>
- [78] Wen P, Gong P, Sun J, *et al.* Design and synthesis of Ni-MOF/CNT composites and rGO/carbon nitride composites for an asymmetric supercapacitor with high energy and power density. *Journal of Materials Chemistry A*, 2015;3(26):13874-13883.  
<https://doi.org/10.1039/c5ta02461g>
- [79] Ding Y, Tang Y, Yang L, *et al.* Porous nitrogen-rich carbon materials from carbon self-repairing g-C<sub>3</sub>N<sub>4</sub> assembled with graphene for high-performance supercapacitor. *Journal of Materials Chemistry A*, 2016;4(37):14307-14315.  
<https://doi.org/10.1039/c6ta05267c>
- [80] Zhu J, Kong L, Shen X, *et al.* Nitrogen-enriched carbon spheres coupled with graphitic carbon nitride nanosheets for high performance supercapacitors. *Dalton Transactions*, 2018;47(29):9724-9732.

- <https://doi.org/10.1039/c8dt01549j>
- [81] Oh T, Kim M, Choi J, *et al.* Design of graphitic carbon nitride nanowires with captured mesoporous carbon spheres for EDLC electrode materials. *Ionics*, 2018;24:3957-3965.  
<https://doi.org/10.1007/s11581-018-2544-0>
- [82] Zhu J, Kong L, Shen X, *et al.* Carbon cloth supported graphitic carbon nitride nanosheets as advanced binder-free electrodes for supercapacitors. *Journal of Electroanalytical Chemistry*, 2020;873:114390.  
<https://doi.org/10.1016/j.jelechem.2020.114390>
- [83] Chen Q, Zhao Y, Huang X, *et al.* Three-dimensional graphitic carbon nitride functionalized graphene-based high-performance supercapacitors. *Journal of Materials Chemistry A*, 2015;3(13):6761-6766.  
<https://doi.org/10.1039/C5TA00734H>
- [84] Shi L, Zhang J, Liu H, *et al.* Flower-like Ni(OH)<sub>2</sub> hybridized g-C<sub>3</sub>N<sub>4</sub> for high-performance supercapacitor electrode material. *Materials Letters*, 2015;145:150-153.  
<https://doi.org/10.1016/j.matlet.2015.01.083>
- [85] Zhang L, Ou M, Yao H, *et al.* Enhanced supercapacitive performance of graphite-like C<sub>3</sub>N<sub>4</sub> assembled with NiAl-layered double hydroxide. *Electrochimica Acta*, 2015;186:292-301.  
<https://doi.org/10.1016/j.electacta.2015.10.192>
- [86] Li L, Qin J, Bi H, *et al.* Ni(OH)<sub>2</sub> nanosheets grown on porous hybrid g-C<sub>3</sub>N<sub>4</sub>/RGO network as high performance supercapacitor electrode. *Scientific Reports*, 2017;7(1):43413.  
<https://doi.org/10.1038/srep43413>
- [87] Shan QY, Guan B, Zhu SJ, *et al.* Facile synthesis of carbon-doped graphitic C<sub>3</sub>N<sub>4</sub>@MnO<sub>2</sub> with enhanced electrochemical performance. *RSC Advances*, 2016;6(86):83209-83216.  
<https://doi.org/10.1039/C6RA18265H>
- [88] Shan QY, Guo XL, Dong F, *et al.* Single atom (K/Na) doped graphitic carbon Nitride@MnO<sub>2</sub> as an efficient electrode material for supercapacitor. *Materials Letters*, 2017;202:103-106.  
<https://doi.org/10.1016/j.matlet.2017.05.061>
- [89] Chang X, Zhai X, Sun S, *et al.* MnO<sub>2</sub>/g-C<sub>3</sub>N<sub>4</sub> nanocomposite with highly enhanced supercapacitor performance. *Nanotechnology*, 2017;28(13):135705.  
<https://doi.org/10.1088/1361-6528/aa6107>
- [90] Guan B, Shan QY, Chen H, *et al.* Morphology dependent supercapacitance of nanostructured NiCo<sub>2</sub>O<sub>4</sub> on graphitic carbon nitride. *Electrochimica Acta*, 2016;200:239-246.  
<https://doi.org/10.1016/j.electacta.2016.03.175>
- [91] Dong B, Li M, Chen S, *et al.* Formation of g-C<sub>3</sub>N<sub>4</sub>@Ni(OH)<sub>2</sub> honeycomb nanostructure and asymmetric supercapacitor with high energy and power density. *ACS Applied Materials & Interfaces*, 2017;9(21):17890-17896.  
<https://doi.org/10.1021/acsami.7b02693>
- [92] Liu L, Wang J, Wang C, *et al.* Facile synthesis of graphitic carbon nitride/nanostructured  $\alpha$ -Fe<sub>2</sub>O<sub>3</sub> composites and their excellent electrochemical performance for supercapacitor and enzyme-free glucose detection applications. *Applied Surface Science*, 2016;390:303-310.  
<https://doi.org/10.1016/j.apsusc.2016.08.093>
- [93] Zhu HL and Zheng YQ. Mesoporous Co<sub>3</sub>O<sub>4</sub> anchored on the graphitic carbon nitride for enhanced performance supercapacitor. *Electrochimica Acta*, 2018;265:372-378.  
<https://doi.org/10.1016/j.electacta.2018.01.162>
- [94] Zhao Y, Xu L, Huang S, *et al.* Facile preparation of TiO<sub>2</sub>/C<sub>3</sub>N<sub>4</sub> hybrid materials with enhanced capacitive properties for high performance supercapacitors. *Journal of Alloys and Compounds*, 2017;702:178-185.  
<https://doi.org/10.1016/j.jallcom.2017.01.125>
- [95] Kavil J, Anjana PM, Periyat P, *et al.* Titania nanotubes dispersed graphitic carbon nitride nanosheets as efficient electrode materials for supercapacitors. *Journal of Materials Science: Materials in Electronics*, 2018;29:16598-16608.  
<https://doi.org/10.1007/s10854-018-9753-1>
- [96] Kavil J, Anjana PM, Periyat P, *et al.* One-pot synthesis of g-C<sub>3</sub>N<sub>4</sub>/MnO<sub>2</sub> and g-C<sub>3</sub>N<sub>4</sub>/SnO<sub>2</sub> hybrid nanocomposites for supercapacitor applications. *Sustainable Energy & Fuels*, 2018;2(10):2244-2251.  
<https://doi.org/10.1039/C8SE00279G>
- [97] Zhang X, Liao H, Liu X, *et al.* Facile synthesis Of Fe<sub>2</sub>O<sub>3</sub> nanospheres anchored on oxidized graphitic carbon nitride as a high-performance electrode material for supercapacitors. *International Journal of Electrochemical Science*, 2020;15(3):2133-

2144.  
<https://doi.org/10.20964/2020.03.54>
- [98] Hou L, Yang W, Xu X, *et al.* In-situ formation of oxygen-vacancy-rich NiCo<sub>2</sub>O<sub>4</sub>/nitrogen-deficient graphitic carbon nitride hybrids for high-performance supercapacitors. *Electrochimica Acta*, 2020;340:135996.  
<https://doi.org/10.1016/j.electacta.2020.135996>
- [99] Guo W, Wang J, Fan C, *et al.* Synthesis of carbon self-repairing porous g-C<sub>3</sub>N<sub>4</sub> nanosheets/NiCo<sub>2</sub>S<sub>4</sub> nanoparticles hybrid composite as high-performance electrode materials for supercapacitors. *Electrochimica Acta*, 2017;253:68-77.  
<https://doi.org/10.1016/j.electacta.2017.09.025>
- [100] Jiang D, Xu Q, Meng S, *et al.* Construction of cobalt sulfide/graphitic carbon nitride hybrid nanosheet composites for high performance supercapacitor electrodes. *Journal of Alloys and Compounds*, 2017;706:41-47.  
<https://doi.org/10.1016/j.jallcom.2017.02.204>
- [101] Ansari SA and Cho MH. Growth of three-dimensional flower-like SnS<sub>2</sub> on g-C<sub>3</sub>N<sub>4</sub> sheets as an efficient visible-light photocatalyst, photoelectrode, and electrochemical supercapacitance material. *Sustainable Energy & Fuels*, 2017; 1(3):510-519.  
<https://doi.org/10.1039/c6se00049e>
- [102] Ansari SA and Cho MH. Simple and large scale construction of MoS<sub>2</sub>-g-C<sub>3</sub>N<sub>4</sub> heterostructures using mechanochemistry for high performance electrochemical supercapacitor and visible light photocatalytic applications. *Scientific Reports*, 2017;7(1):43055.  
<https://doi.org/10.1038/srep43055>
- [103] Ragupathi V, Panigrahi P and Subramaniam NG. g-C<sub>3</sub>N<sub>4</sub> doped MnS as high performance electrode material for supercapacitor application. *Materials Letters*, 2019;246:88-91.  
<https://doi.org/10.1016/j.matlet.2019.03.054>
- [104] Chen X, Zhu X, Xiao Y, *et al.* PEDOT/g-C<sub>3</sub>N<sub>4</sub> binary electrode material for supercapacitors. *Journal of Electroanalytical Chemistry*, 2015; 743:99-104.  
<https://doi.org/10.1016/j.jelechem.2015.02.004>
- [105] Zhou SX, Tao XY, Ma J, *et al.* Synthesis of flower-like PANI/g-C<sub>3</sub>N<sub>4</sub> nanocomposite as supercapacitor electrode. *Vacuum*, 2018;149:175-179.  
<https://doi.org/10.1016/j.vacuum.2017.12.019>
- [106] Li F, Dong Y, Dai Q, *et al.* Novel freestanding core-shell nanofibrillated cellulose/polypyrrole/tubular graphitic carbon nitride composite film for supercapacitors electrodes. *Vacuum*, 2019;161:283-290.  
<https://doi.org/10.1016/j.vacuum.2018.12.046>
- [107] Xie H, Guo Z, Wang M, *et al.* Facile fabrication of PANI/g-C<sub>3</sub>N<sub>4</sub>/MXene composites as electrode materials for supercapacitors. *New Journal of Chemistry*, 2023;47(18):8670-8678.  
<https://doi.org/10.1039/D3NJ00943B>
- [108] Alshahrie A and Ansari MO. High Performance Supercapacitor Applications and DC Electrical Conductivity Retention on Surfactant Immobilized Macroporous Ternary Polypyrrole/Graphitic-C<sub>3</sub>N<sub>4</sub>@Graphene Nanocomposite. *Electron. Mater. Lett.* 15, 238–246 (2019).  
<https://doi.org/10.1007/s13391-018-00107-6>
- [109] Vattikuti SVP, Reddy BP, Byon C, *et al.* Carbon/CuO nanosphere-anchored g-C<sub>3</sub>N<sub>4</sub> nanosheets as ternary electrode material for supercapacitors. *Journal of Solid State Chemistry*, 2018;262:106-111.  
<https://doi.org/10.1016/j.jssc.2018.03.019>
- [110] Zhang J, Ding J, Li C, *et al.* Fabrication of novel ternary three-dimensional RuO<sub>2</sub>/graphitic-C<sub>3</sub>N<sub>4</sub>@reduced graphene oxide aerogel composites for supercapacitors. *ACS Sustainable Chemistry & Engineering*, 2017;5(6):4982-4991.  
<https://doi.org/10.1021/acssuschemeng.7b00358>
- [111] Ma J, Tao XY, Zhou SX, *et al.* Facile fabrication of Ag/PANI/g-C<sub>3</sub>N<sub>4</sub> composite with enhanced electrochemical performance as supercapacitor electrode. *Journal of Electroanalytical Chemistry*, 2019;835:346-353.  
<https://doi.org/10.1016/j.jelechem.2018.12.025>
- [112] Adan W, Cochran EW, Zulfiqar S, *et al.* Wet-chemical engineering of Ag-BiVO<sub>4</sub>/Bi<sub>2</sub>S<sub>3</sub> heterostructured nanocomposite on graphitic carbon nitride (g-C<sub>3</sub>N<sub>4</sub>) sheets for high performance supercapacitor application. *Journal of Energy Storage*, 2023;72:108416.  
<https://doi.org/10.1016/j.est.2023.108416>
- [113] Parveen S, Cochran EW, Zulfiqar S, *et al.* Iron/

- vanadium co-doped tungsten oxide nanostructures anchored on graphitic carbon nitride sheets (FeV-WO<sub>3</sub>@g-C<sub>3</sub>N<sub>4</sub>) as a cost-effective novel electrode material for advanced supercapacitor applications. *RSC Advances*, 2023;13(38):26822-26838.  
<https://doi.org/10.1039/D3RA04108E>
- [114] Zhang S, Huang Y, Wang J, *et al.* Ti<sub>3</sub>C<sub>2</sub>T<sub>x</sub>/g-C<sub>3</sub>N<sub>4</sub> heterostructure films with outstanding capacitance for flexible Solid-state supercapacitors. *Applied Surface Science*, 2022;599:154015.  
<https://doi.org/10.1016/j.apsusc.2022.154015>
- [115] Li J, Zhang X, Li X, *et al.* Highly transparent and flexible graphitic C<sub>3</sub>N<sub>4</sub> nanowire/PVA/PEDOT: PSS supercapacitors for transparent electronic devices. *Functional Materials Letters*, 2020;13(02):2051006.  
<https://doi.org/10.1142/S1793604720510066>
- [116] Wang Y, Liu L, Ma T, *et al.* 2D graphitic carbon nitride for energy conversion and storage. *Advanced Functional Materials*, 2021;31(34):2102540.  
<https://doi.org/10.1002/adfm.202102540>
- [117] Jasna M, Pillai MM, Abhilash A, *et al.* Polyaniline wrapped carbon nanotube/exfoliated MoS<sub>2</sub> nanosheet composite as a promising electrode for high power supercapacitors. *Carbon Trends*, 2022;7:100154.  
<https://doi.org/10.1016/j.cartre.2022.100154>
- [118] Zhao Y, Hao H, Song T, *et al.* MnO<sub>2</sub>-graphene based composites for supercapacitors: synthesis, performance and prospects. *Journal of Alloys and Compounds*, 2022;914:165343.  
<https://doi.org/10.1016/j.jallcom.2022.165343>